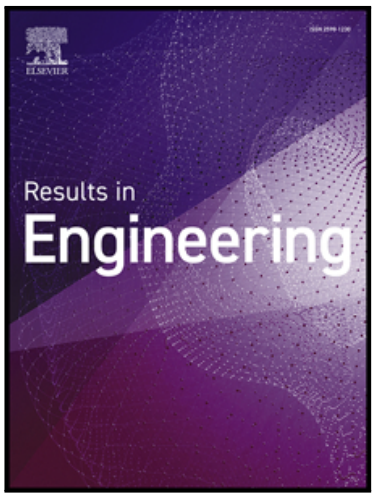

Energy Optimization of a Dish/Stirling Solar System for Electricity Generation

Ghislain Junior Bangoup Ntegmi , Germaine Mabou Ninkam , Francois Lanzetta , Flavian Emmanuel Sapnken , Mebarek-Oudina Fateh , Bleck Fredi Kamto Pomou , René Tchinda

PII: S2590-1230(25)04545-1
DOI: https://doi.org/10.1016/j.rineng.2025.108501
Reference: RINENG 108501

To appear in: *Results in Engineering*

Received date: 1 August 2025
Revised date: 5 November 2025
Accepted date: 28 November 2025

Please cite this article as: Ghislain Junior Bangoup Ntegmi , Germaine Mabou Ninkam , Francois Lanzetta , Flavian Emmanuel Sapnken , Mebarek-Oudina Fateh , Bleck Fredi Kamto Pomou , René Tchinda , Energy Optimization of a Dish/Stirling Solar System for Electricity Generation, *Results in Engineering* (2025), doi: https://doi.org/10.1016/j.rineng.2025.108501

Highlights

From this analysis, the main contributions follow:

- A maximum electrical output of 10.85 kW is achieved at T_E=400K.
- A solar electric energy yield of 43.78% is achieved at an optimum frequency of 18Hz.
- Electrical power, energy efficiency, internal thermal losses, regenerator inefficiency and gas spring hysteresis are discussed.
- Heat loss due to the regenerator's imperfection is the highest in the Dish/Stirling system, at 0.520 kW.

Energy Optimization of a Dish/Stirling Solar System for Electricity Generation

Ghislain Junior Bangoup Ntegmi[1,2*], Germaine Mabou Ninkam[1,3], Francois Lanzetta[4], Flavian Emmanuel Sapnken[5], Mebarek-Oudina Fateh[6], Bleck Fredi Kamto Pomou[1], René Tchinda[7,8]

[1]Energy, Electrical Systems and Electronics Laboratory, Department of physics, University of Yaounde I, Yaounde PO Box 812, Cameroon.

[2]Carnot Energy Laboratory (CEL), Department of Physics, Faculty of Science, University of Bangui, Bangui, PO Box 1450, Central African Republic.

[3]Laboratory of Materials Analysis, Local Materials Promotion Authority, Yaounde, Cameroon

[4]FEMTO-ST Institute, Univ. Bourgogne Franche-Comte, CNRS Parc technologique, 2 avenue Jean Moulin, F-90000 Belfort, France

[5]Laboratory of Technologies and Applied Science, University Institut Technologie of Douala, PO Box 8698, Cameroon

[6]Deparment of Physics, Faculty of Sciences, University of 20 Août 1955-Skikda, Skikda 21000, Algeria

[7]Laboratory of Mechanical and Modelisation of Physical systems, Department of Physics, University of Dschang, PO Box 67, Dschang, Cameroon

[8]Industrial and Energy Systems Engineering laboratory, University institute of Technology Fotso Victor, University of Dschang, PO Box 134, Bandjoun

*Corresponding author: email: ghislain.bangoup@facsciences-uy1.cm (Ghislain Junior Bangoup Ntegmi)

Orcid : https://orcid.org/0009-0007-1485-8226 (Ghislain Junior Bangoup Ntegmi)

Highlights

- A maximum electrical output of 10.85 kW is achieved at T_E=400K.
- A solar electric energy yield of 43.78% is achieved at an optimum frequency of 18Hz.
- Electrical power, energy efficiency, internal thermal losses, regenerator inefficiency and gas spring hysteresis are discussed.
- Heat loss due to the regenerator's imperfection is the highest in the Dish/Stirling system, at 0.520 kW.

Abstract

Stirling cycle machines are used in both motor and receiver cycles. The Stirling cycle engine has good potential for use due to advantages such as external combustion and fuel flexibility. This study presents a Dish/Stirling system to capture solar energy for electricity generation by optimizing its energy performance. The system comprises a solar collector to convert solar energy into heat, a Stirling engine to convert heat into mechanical energy, and an alternator to convert mechanical energy into electrical energy. The Schmidt model with imperfect regeneration is used, taking into account work losses due to gas spring hysteresis. In addition, thermal losses from the solar collector are taken into account in this model. Numerical

modeling was performed using MATLAB software. The impact of operational and design elements on the energy performance of the system are studied. Two objective functions were studied, namely solar electric power and solar electric energy efficiency. The results reveal that the present Dish/Stirling explores an improvement in solar electric energy efficiency of 7% in particular in the absence of consideration of fluid friction losses. Optimum solar electric energy yield is 43.78% at f=18Hz, a maximum electrical power is 10.85 kW at T_E=400K. Finally, the heat loss due to regenerator imperfections is greatest for the paraboloidal concentrator, with a value of 0.520 kW, while the smallest loss is that due to gas spring hysteresis, with a value of 0.045 kW. This system can be used for lighting in non-electrified areas.

Key words: Stirling cycle; Dish/Stirling; Electricity; Thermal losses; Energy performance.

1. Introduction

Faced with the disastrous environmental consequences of fossil fuels, the search for alternative technological solutions has become an absolute priority. The sun, an abundant and renewable source of energy, is at the heart of sustainable development strategies for a cleaner, safer energy future. Thermodynamic solar power is an energy technology that harnesses the photothermal conversion of solar energy into electricity, using concentration and thermodynamic conversion systems. Thermodynamic solar power converts solar energy into heat, which is then used to turn a turbine and generate electricity, as well as to provide heat for industry. What sets the Dish/Stirling system apart from other concentrated solar power systems is its modular design, which makes it particularly suitable for small-scale power generation, offering a flexible and efficient solution. In an earlier study, Nassar et al. [1] proposed an innovative hybrid energy system, integrating Dish/Stirling concentrating solar technology and anaerobic biomethanization, to meet Libya's energy needs while reducing greenhouse gas (GHG) emissions and promoting a circular, sustainable economy. The energy assessment shows that the hybrid system will generate 5,670,534 kWh of electricity annually, with a maximum capacity of 1,230 MW, enhancing energy reliability. The project requires initial financing of $12.365 million, with a competitive energy cost and payback period of 20.04 years, reducing CO_2 emissions by 7.8 kilotonnes per year [1]. A study by Khawaldeh et al. evaluated and compared the energy and economic performance of the national grid power supply and the Dish/Stirling energy generation system for a residential building in Mafraq, Jordan. The results of the study highlight the potential of the Dish/Stirling system as a reliable energy solution, capable of generating electricity efficiently even under adverse climatic and environmental conditions [2]. Depending on their operational architecture, Stirling thermomechanical conversion systems can be categorized into free piston and crank/kinematic devices and [3]. In the kinematically linked Stirling machine, the fluctuating dynamic pressure of the working fluid is converted into mechanical energy via an articulated motion conversion mechanism, which links the mutually moving elements, notably the displacer and the power piston, within the engine enclosure. The Free Piston Stirling Engine (FPSE) replaces the conventional transmission system with a set of internal springs coupled to the displacer and power piston, thus eliminating kinematic linkage mechanisms. The movement of the moving parts is then governed solely by fluctuations in the dynamic pressure of the working fluid, giving this type of motor significant advantages, including longer service

life, reduced acoustic noise, elimination of maintenance operations, minimized vibration, autonomous starting and high thermodynamic efficiency [3, 4]. Because of its intrinsic advantages, FPSE technology is particularly suitable for a variety of applications, including solar energy conversion systems (Dish/Stirling) [5], cryocoolers [6] and micro-electric and thermal cogeneration systems (micro-CHP). The latter system enables simultaneous production of electricity and heat from the same energy source, and compact units (micro-CHP) have been available for domestic applications for some years now [7]. In addition, the free piston Stirling engine (FPSE) is the main industrial unit used for solar power generation. Its design and manufacturing challenges include start-up (a necessary condition), which can be difficult due to the need to reach a certain level of temperature and pressure to initiate the heat cycle. But preheating systems, such as the use of auxiliary heat sources, can be integrated to facilitate this start-up phase. Obtaining a stable limit cycle in its dynamics (sufficient condition) is also a challenge, because for this engine to operate efficiently, it must reach a stable limit cycle, where temperature and pressure conditions remain constant despite load variations [8]. As a result, its design must take into account thermal management and gas dynamics. And this can include optimizing heat exchangers to ensure efficient heat transfer between the gas and the surrounding media. Also dynamics control for the adjustment of operating parameters, such as rotational speed and piston geometry, to maintain cycle stability [9]. Finally, the use of materials capable of withstanding temperature variations without deforming, to guarantee engine reliability and durability [10]. Coupled with solar dishes, free-piston Stirling engines play a crucial role in the efficiency and durability of Dish/Stirling systems. Their innovative designs and performance advantages make them a preferred choice for renewable energy applications [11]. Tursunović et al.[12] have designed an innovative receiving system for a concentrated solar power plant, in collaboration with the Polytechnic Institute of Turin, incorporating Dish/Stirling solar energy harvesting technology to provide heat in the form of hot water, even during periods of low solar radiation. The results show that life-cycle analysis reveals that Dish/Stirling technology has a significantly lower carbon footprint, with emissions of 5,332.8 kg CO_2 eq. during production of its basic components, compared with 12,240 kg CO_2 eq. for a conventional device during its operating phase. Researchers have carried out an in-depth study into the energy efficiency of a solar system, using the NSGAII algorithm to improve the thermal and economic performance of a motor, identifying key factors for optimal design [13]. Further research has explored the application of the Stirling engine and its thermodynamic process to improve energy efficiency. To optimize a vehicle's thermal management, a team of researchers led by Bani-Hani [14] carried out an innovative study integrating a Stirling energy conversion module into the cooling system, enabling efficient pressure regulation. Accurate meteorological data at the installation site is crucial for optimizing the performance of the Dish/Stirling system, guaranteeing its efficiency and reliability [15]. Several predictive approaches have been developed to estimate total daily solar irradiance in different regions [16, 17]. In addition, further research has examined the potential of Stirling technology to generate electricity by exploiting its innovative thermodynamic cycle. Table 1 provides a concise overview of existing work and its shortcomings.

The main objective of this research is to evaluate the energy performance of a parabolic concentrator solar system for electricity generation in the commune of BAZOU, Cameroon, with a view to exploiting local renewable energy resources. A comprehensive mathematical model has been developed to simulate the complex interactions between the key components of a Dish/Stirling system, including the solar receiver, solar concentrator and Stirling engine, in order to optimize the system's energy performance. Schmidt's non-ideal regeneration

method has been applied to model the thermodynamic cycle of the Stirling engine, allowing real losses to be taken into account. Numerical simulation was carried out using a customized Matlab program. The objective functions of the electric Dish/Stirling, in particular efficiency and electrical power, were analyzed and quantified. Optimum specifications for use are defined on the basis of key parameters. Following the introduction, the next section presents the methods and materials used. In brief, the results and discussion highlight the detailed analysis of the operational and geometric characteristics of the solar collector and Stirling engine, influencing the electrical performance of the Dish/Stirling device.

The solutions provided by this research can be used to optimize the power supply to the commune of BAZOU, by offering a reliable alternative to the frequent power interruptions provided by ENEO Cameroun [18]. The major contributions of this analysis are as follows:

- The impacts of frequencies, porosities, internal lengths, internal diameter of the Stirling engine, surface area of the concentrator and solar receiver, ambient temperature and irradiation on device performance are measured.
- High Dish/Stirling energy efficiency is achieved through the optimal elements obtained.
- Optimal operating parameters lead to improved electrical performance of the Dish/Stirling device
- The impact of heat loss on the Dish/Stirling's energy performance needs to be discussed.

Dish/Stirling systems only work in clear skies, and must be used in hybrid with other clean electricity production systems such as parabolic troughs or photovoltaics to supply the BAZOU commune.

Table 1: Overview of studies carried out and their shortcomings.

Study	Year	Brief description	Solar technology category	How much heat loss is considered?	How many design criteria and operational variables are defined?	Does the system emit CO_2?	How many target functions are examined?	P_{elec} (kW)	η_{elec} (%)
This work				**6**	**13**	**No**	**2**	**10.85**	43.78
Khosravi et al. [19]	2019	The artificial intelligence approach (MLP-PSO, GMDH, MLP-GA,	Dish/Stirling	3	5	No	2	2	25

		ANFIS-PSO and ANFIS-GA) is used to model a Dish/Stirling solar device.							
Zayed et al. [20]	2020	A new Dish/Stirling Solar System (SDSS) with a nominal output of 25 kW is experimentally implemented and thermodynamically modeled.	Dish/Stirling	3	7	No	3	25	19.55
Nsafon et al. [21]	2020	A hybrid photovoltaic/wind/diesel system is simulated with HOMER software to supply the consumption of a housing estate of 4,476.5 kWh.	PV/wind/diesel hybrid system	-	-	Yes	3	700, 350 and 350	20
Zayed et al. [22]	2021	Modeling a Dish/Stirling Solar System (SDSS) using opto-geometric sizing is designed to calculate its electricity production and overall efficiency. With SDSS diameters of 2.5 m.	Dish/Stirling	3	5	No	2	0.735	17.1
Allouhi et al. [23]	2022	Multi-objective optimization is used to design	Dish/Stirling	3	4	No	2	100	22.99

		the most cost-effective and energy-efficient Dish/Stirling (SDS) power plant. The technical-economic evaluation of a 10 MW power plant using the NSGA II genetic algorithm was adopted.								
Tong et al. [24]	2023	The authors propose a new STPG S-CO 2 system integrated with the Rankine Steam (SR) cycle. The SR cycle absorbs waste heat from the S-CO2 Brayton cycle, and the introduction of the SR cycle can optimize the solar power utilization rate. Steam turbine inlet temperature and pressure are 600 ^{o}C/30 MPa from the SR cycle.	Solar Tower	-	1	Yes	1	-	34.4	
Alhawsawi et al. [25]	2023	Given the many advantages of the Dish/Stirling system, this research	Dish/Stirling	3	3	No	2	3.903	20.92	

		proposes in-depth theoretical modelling and performance evaluation of a hybrid system for the combined production of electricity, heat and drinking water using Dish/Stirling technology for single-effect distillation (SHPS-DS), with the aim of optimizing tri-generation.							
Faheem et al. [26]	2024	The specialists present an abridged study of the design, numerical simulation and implementation of a CSP system. During the design phase, the collector opening area of the solar parabolic trough was set at 1.5 m^2 with a width of 1 m and a length of 1.5 m. With Tamb=20.54 K, an N-S direction of 10:00.	Parabolic trough solar collectors	3	1	No	2	1.035	30.48

Choukri et al. [27]	2024	The researchers in this work, analyze the potential of a Step Energy Storage (SSP) system to reduce the electricity consumption of a rural community in Ain Beni Mathar, through optimized load management and the use of high-precision data.	Dish/Stirling	3	3	No	1	10	-
Zayed et al. [28]	2025	The design details and experimental results of the TJ-SDSS parabolic trough solar system in Tianjin are presented in this study.	Tianjin solar dish-Stirling system (TJ-SDSS)	3	4	No	2	23.45	23.5%

2. Material and methods

2.1 Study area and machine description

The commune of BAZOU, located in the western part of Cameroon, in the NDE department, is characterized by a humid tropical climate. It covers an area of 249 km^2, and is home to around 32,000 people. According to meteorological records, average solar intensity per hour fluctuates between 2 and 2.7 $kWh.m^{-2}$ during periods of low insolation, and between 5.2 and 5.8 $kWh.m^{-2}$ during periods of high insolation, as highlighted in the Ref [29] study on predicting direct solar irradiation. The map of this commune is shown in Fig 1. Table 2 shows the geographical data and climatic characteristics of the study site.

Table 2: The geographic data of the site

Position studied	Latitude	Longitude	Altitude	Climate	Albedo

	(°)	(°)	(m)		
BAZOU	5.063	10.469	1250	monsoon	0.2

The machine studied is a hybrid system combining a Dish-type solar concentrator with a Stirling engine and alternator to generate electricity. A schematic representation of this device is shown in Fig 2. This model is made up of four main components, corresponding to the five key parameters defined in the past. Helium is used as a heat transfer gas and treated as a perfect fluid.

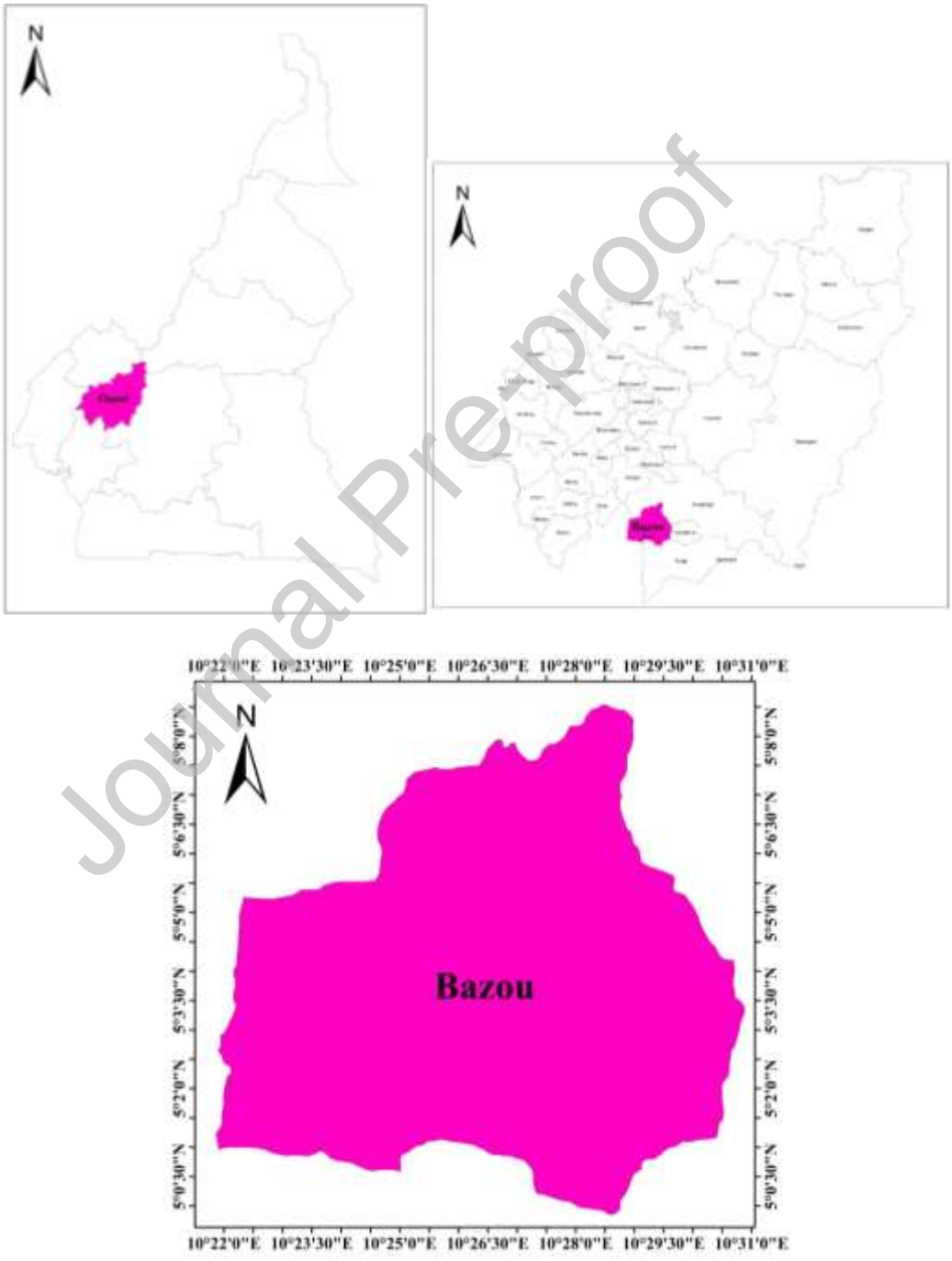

Fig 1: BAZOU area.

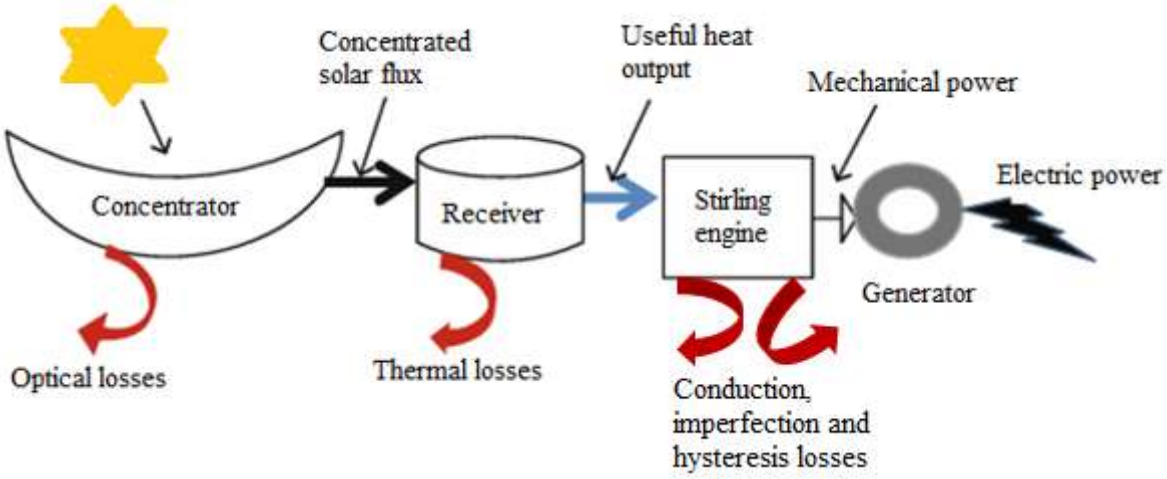

Fig 2: Electricity production diagram for Dish/Stirling technology.

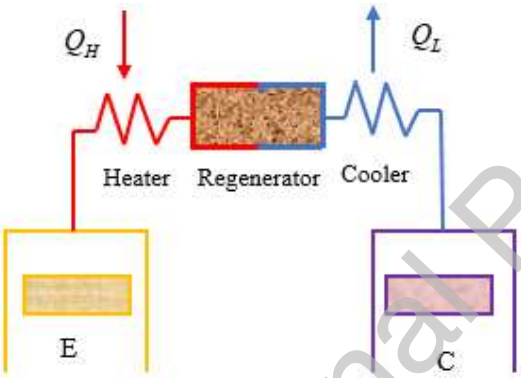

Fig 3: Internal components of the Stirling engine.

2.2 Methodology

2.2.1 Thermodynamic analysis of the Dish/Stirling system

The Stirling solar equipment is an innovative system that converts the sun's radiant energy into electricity. The receiver captures this concentrated solar energy and converts it into heat, which in turn raises the temperature of the helium used as the technical gas in Stirling engine. The stages in the Stirling engine's operating cycle can be seen in Fig 3. The heat produced at high temperature is converted into mechanical energy by the Stirling engine. This mechanical energy is then converted into electrical energy via an alternator, generating electricity. Mathematical models derived from Ref [30, 31] have estimated the thermodynamic properties of air, helium and hydrogen. A sophisticated numerical approach simulates the thermal behavior of the Stirling energy system. The selection of helium as the active agent optimizes energy efficiency, surpassing the thermodynamic characteristics of air but less than the use of hydrogen as demonstrated in the analysis of Ref [32], specific to Stirling engine

applications. Since helium optimizes the reverse Stirling cycle more, hydrogen optimizes the Stirling cycle better.

2.2.1.1 Solar dish collector

An advanced solar concentration system, incorporating dynamic tracking, channels the rays to a high-efficiency receiver. It is then converted into thermal energy to raise the temperature of the Stirling engine's expansion chamber. Previous researches [33, 34], reveals that the thermal energy required by a parabolic solar mirror is modelled by Eq (1), including energy losses (radiation, conduction, convection).

$$\dot{Q}_u = IA_{app}\eta_0 - A_{rec}\left[h\left(T_{ab} - T_{amb}\right) + \varepsilon\delta\left(T_{ab}^4 - T_{amb}^4\right)\right] \quad (1)$$

The energy efficiency η_0 of the parabolic receiver, calculated using Eq (2), represents the proportion of solar energy captured relative to total irradiation [33, 35].

$$\eta_c = \frac{\dot{Q}_u}{IA_{app}} = \eta_0 - \frac{1}{IC}\left[h\left(T_{ab} - T_{amb}\right) + \varepsilon\delta\left(T_{ab}^4 - T_{amb}^4\right)\right] \quad (2)$$

With a given energy efficiency η_0, the temperature of the absorbing element T_{ab} can be defined using Eq (2), based on various levels of direct solar irradiation and the concentration factor $C=A_{app}/A_{rec}$.

A reformulation of this equation can be made to explicitly integrate the thermal variable, as follows [36].

$$\rho \cdot V \cdot C_p \frac{dT_{ab}}{dt} = \dot{Q}_u \quad (3)$$

where C_P, V, ρ is the thermal capacity of the ceramic wall, volume and density respectively.

Relation (3) simulates the thermal evolution of the air in the solar absorber as a function of time. In other words, this equation simulates the thermal evolution of the air in the solar absorber, not the absorber walls. The “ceramic walls” mentioned refer to the material making up the solar absorber, not to the air it contains. Eq (3) simulates how the temperature of the air in the absorber varies as a function of time, taking into account the heat capacity (C_P), volume (V) and density (ρ) of the absorber wall. In other words, although the equation concerns the evolution of air temperature, it uses the thermal properties of the absorber wall to determine how this temperature changes with time.The heat is then transferred to the heat transfer fluid in the hot zone of the Stirling engine. This requires calculation of the fluid temperature in the absorber tubes, received by Eq (4) [36].

$$T_f(t) = T_{ab}(t) - \frac{\dot{Q}_u}{h_f \cdot A_{rec}} \quad (4)$$

2.2.1.2 Modeling of the Stirling engine

Stirling engine operation is simulated using Schmidt's theoretical approach, which enables its performance to be predicted as a function of its configuration. This analytical method,

described in Ref [37, 38], offers an advanced mathematical tool. The analysis incorporates simplifying assumptions [39] and heat losses related to the regenerator and gas springs, calculated separately and integrated with Smith's results [40] to improve accuracy. Compression and expansion volume variations are modeled by Eq (5) and (6), which describe sinusoidal kinematics as a function of phase shift, angular velocity and cycle period [41, 42].

$$V_E = V_{em} + \frac{V_{eb}}{2}\left(1+\cos(\alpha+\chi)\right) \tag{5}$$

$$V_C = V_{cm} + \frac{V_{cb}}{2}\left(1+\cos(\alpha)\right) \tag{6}$$

where $\chi, V_C, V_E, V_{cm}, V_{em}, V_{cb}, V_{eb}$ denote angular phase shift, cold and hot chamber capacities, inactive compression and expansion volumes, and corresponding sweep volumes, respectively.

With $\alpha = \psi_0 \cdot t$ (7)

The remaining volumes remain stable. The total quantity of helium in the Stirling engine is observed by summing up the quantities present in each compartment, giving a constant value represented by Eq (8) [43].

$$m_C + m_h + m_R + m_k + m_E = m \tag{8}$$

Total engine pressure is determined by fluctuating temperatures, mass volumes and the perfect gas constant, according to Eq (9) [44, 45] :

$$P = m \cdot R \left(\frac{V_E + V_h}{T_E} + \frac{V_R}{T_R} + \frac{V_C + V_k}{T_C} \right)^{-1} \tag{9}$$

According to relation (10) [46], the regenerator capacity can be calculated by.

$$V_R = A_{mat} \cdot \psi \cdot L_R \tag{10}$$

Eq (11) describes the ratios of inactive volume, displaced volume and compression temperature.

$$\mathrm{x} = \frac{V_{cm}}{V_{em}}, \quad K = \frac{V_{cb}}{V_{eb}} \text{ and } \tau = \frac{T_C}{T_E} \tag{11}$$

The division of the Stirling engine into three sections implies that helium temperatures are equal in the heating and expansion zones, as well as in the cooling and compression zones, as shown in relationship (12).

$$T_h = T_E = T_f \text{ then } T_k = T_C \tag{12}$$

The fluid temperature on the cold side (T_C) exceeds the ambient temperature (T_{amb}) to allow dissipation, contrary to the model's assumptions, which target the theoretical ideal and not real exchanges.

Consequently, the regeneration temperature is assumed to be constant and to vary linearly, according to formula (13) [47, 48].

$$T_r = \frac{T_E - T_C}{\ln\left(\frac{T_E}{T_C}\right)}$$

(13)

At 1500 rpm, the efficiency produced by the Stirling cycle combines the efforts of the cylinders [49, 50] :

$$W_i = W_E + W_C$$

(14)

$$Q_{h,i} = W_E = -\oint P dV_E$$

(15)

$$Q_{k,i} = W_C = -\oint P dV_C$$

(16)

The regenerator's internal heat losses, caused by the temperature gradient between the walls, are evaluated as follows [49]:

$$Q_{cd} = \frac{\lambda_w \cdot A_{wg}}{f \cdot l_R}\left(T_E - T_C\right)$$

(17)

The regenerator's thermal inefficiencies cause energy loss, which can be calculated using Eq (18) [50, 51, 52].

$$Q_{imp} = mC_p\left(1-\eta_{reg}\right)\left(T_E - T_C\right)$$

(18)

The hysteresis losses of gas springs are simulated by Eq (19) [53, 54], illustrating the accumulation and restitution of energy by the working fluid during compression and expansion cycles.

$$W_{hys} = \sqrt{\frac{1}{32}\omega\gamma^3(\gamma-1)T_w P_{mean} k_g (\frac{V_d}{2V_t})^2 A_{wg}}$$

(19)

- **Stirling engine performance**

The required input power is determined by summing the energy losses and the isothermal Schmidt power, according to [55, 56].

$$\dot{W} = \dot{W}_i + \dot{W}_{loss}$$

(20)

Efficiency is calculated as the ratio between the mechanical energy generated and the external heat absorbed by the engine, according to (21) [29, 56, 57].

$$\eta_{eng} = \frac{|\dot{W}|}{Q_h + Q_{loss}} \quad (21)$$

Numerical simulation of the Dish/Stirling system is based on simplifying assumptions that can affect accuracy. The approximations concern solar concentration and heat losses, as well as the Schmidt model for the Stirling engine. These deviations can lead to discrepancies between predicted and actual performance. Environmental fluctuations and component degradation contribute to these discrepancies. To obtain reliable simulations, it is essential to refine the numerical models to reflect the actual operating conditions of the solar energy system and thus improve the accuracy of the results. This requires more accurate modeling.

Fuel flexibility in Stirling engines, particularly with perfect gases such as hydrogen, helium and air, is crucial for several reasons. These substances enhance thermal performance thanks to their superior thermophysical characteristics. The use of these fluids enables application versatility, giving engines significant operational flexibility. What's more, atmospheric air reduces energy costs thanks to its unlimited availability. The use of clean fuels such as hydrogen contributes to the reduction of anthropogenic emissions, ensuring stability and reliability at the same time. This versatility fosters technological innovation, reinforcing the role of Stirling engines in contemporary energy systems.

2.2.2 Performance of the Dish/Stirling solar electric system

The Dish/Stirling system is described by several equations for evaluating its performance. Eq (22) [58] and (23) [59, 60] determine the energy yield and solar electric power of the Dish/Stirling, respectively.

$$\eta_{elec} = \eta_c \cdot \eta_{eng} \cdot \eta_{GE} \quad (22)$$

$$P_{elec} = \eta_{elec} I \cdot A_{app} \quad (23)$$

Tableau 3 : Technical specifications

Concentrator system	Paraboloid 12 seg [36, 58, 61]
C	1300
ε	0.9
η_0 (%)	90
h (W.m^{-2}.K^{-1})	20
δ (W.m^{-2}.K^{-4})	5.67x10^{-8}
T_{ab} (K)	1100
Stirling engine	Alpha solo 161 [30, 36]
Working gas	Helium
f (Hz)	25

T_{amb} (K)	288
χ	90°
Regenerator	
kg ($W.K^{-1}.m^{-1}$)	10
$d_R(m)$	$3x10^{-3}$
L_R(m)	$6x10^{-2}$
ψ	0.7
Cooling	
T_C (K)	288
V_{cb} (cm^3)	160
Vcm (cm3)	22
Heating	
T_E (K)	320
Veb (cm3)	160
Vem (cm3)	28.06
Vcm (cm3)	28.06

2.2.3 Objective functions and description of the optimization method

Previous research focused mainly on optimizing energy performance, neglecting other key criteria. In this study, each objective is either maximized or minimized, and all are equivalent in the decision-making process. Priorities vary according to the specific needs of the designer. So the optimal selection network for a Stirling cycle machine is not a single approach, but rather a set of constraints and criteria applied to Stirling engine design and evaluation. The aim is to find the best combination of parameters to meet performance targets, such as efficiency, power and reliability, while taking into account physical and economic constraints. The Dish/Stirling optimization approach is based on the use of evolutionary algorithms to solve complex multi-objective problems. This strategy systematically explores the solution space and identifies parameter combinations that simultaneously improve energy efficiency and power output.

- **Constraints**

Fourteen key factors linked to the architectural structure and the process of focusing the sun's rays were chosen to improve the energy performance of the Dish/Stirling system. These elements are detailed below:

$$288 \le T_{amb} \le 303K \quad (24)$$

$$200 \le I \le 800Wh.m^{-2} \quad (25)$$

$$500 \le T_{ab} \le 1100K \quad (26)$$

$$300 \le T_E \le 400K \quad (27)$$

$$200 \le T_C \le 300K \quad (28)$$

$$54 \le A_{app} \le 60Cm^2 \quad (29)$$

$$5 \le A_{rec} \le 20Cm^2 \quad (30)$$

$$50 \le d_R \le 100mm \quad (31)$$

$$10 \le f \le 50Hz \quad (32)$$

$$10 \le l_R \le 50mm \quad (33)$$

$$0.6 \le \eta_0 \le 0.9 \quad (34)$$

$$1 \le K \le 1.3 \quad (35)$$

$$0.5 \le \psi \le 1 \quad (36)$$

$$0.6 \le \varepsilon \le 0.9 \quad (37)$$

- **Optimization criteria**

The criteria used for optimization include:

- *Maximum Electrical Power:* The configuration should aim to maximize the electrical power produced by the Dish/Stirling device.
- *Energy Efficiency:* The efficiency of the solar concentrator should be maximized, measured as the percentage conversion of solar energy into electrical energy.

Optimizing a Dish/Stirling system requires synergy between the key components. *The collection area of the parabolic reflector* determines the energy density at focus, thus impacting thermodynamic efficiency. *Stirling engine parameters* such as piston stroke, compression ratio and thermal management must be calibrated to maximize the conversion of radiative energy into mechanical energy. *Dynamic operating ranges* must be adjusted to compensate for environmental fluctuations, ensuring maximum and stable power production.

Precise numerical simulation enables these parameters to be fine-tuned, guaranteeing the sustainability, operational reliability and economic profitability of the solar energy system.

To define the ideal device settings, a computational model was developed using the Matlab programming language and the evolutionary optimization method.

2.3 Numerical resolution procedure, convergence criteria, computer details and validation of the MATLAB model details

The model begins by establishing the equations governing the Dish/Stirling system, including energy conservation equations, Stirling cycle thermodynamics and heat losses. These equations are coded in MATLAB, where input parameters such as initial conditions and material properties are defined. Runge-Kutta methods, tables of integrals from (Dwight 1961) and Fourier series are used to integrate the differential equations. Simulations are carried out for different scenarios, varying the input conditions. Fig 4 summarizes the overall process and the mathematical operations involved.

- **Convergence criteria**

A convergence criterion is defined to stop iterations when the relative variation in electrical power or efficiency is below a predefined threshold (e.g. 1%). Convergence is validated by checking that the results no longer change significantly as the number of iterations or time steps increases.
Ensuring the reliability of simulation results requires specifying the characteristics of the equipment used, as well as the specifics of the computer program.

- **Hardware specifications**

- Recommended processor: Intel Core i7 (or equivalent) with a clock speed of at least 3.0 GHz.
-RAM: 16 GB or more recommended for intensive calculations
-Storage requirements: 512 GB SSD for fast loading and access times.
-System environment: Windows 10 or Linux (Ubuntu 20.04 minimum) recommended for MATLAB

- **Model runtime**

Processing time depends on the parameters set. The time steps, ranging from 0.1 to 25, gave execution times varying from 1h30 to 30 minutes for the complete program.

- **Validation of the MATLAB model details**

Numerical results are compared with experimental data available in the literature. Errors between simulations and experimental data are calculated to validate the model. Sensitivity analyses are also carried out to assess the impact of variations in input parameters on the results, thus confirming the robustness of the model.

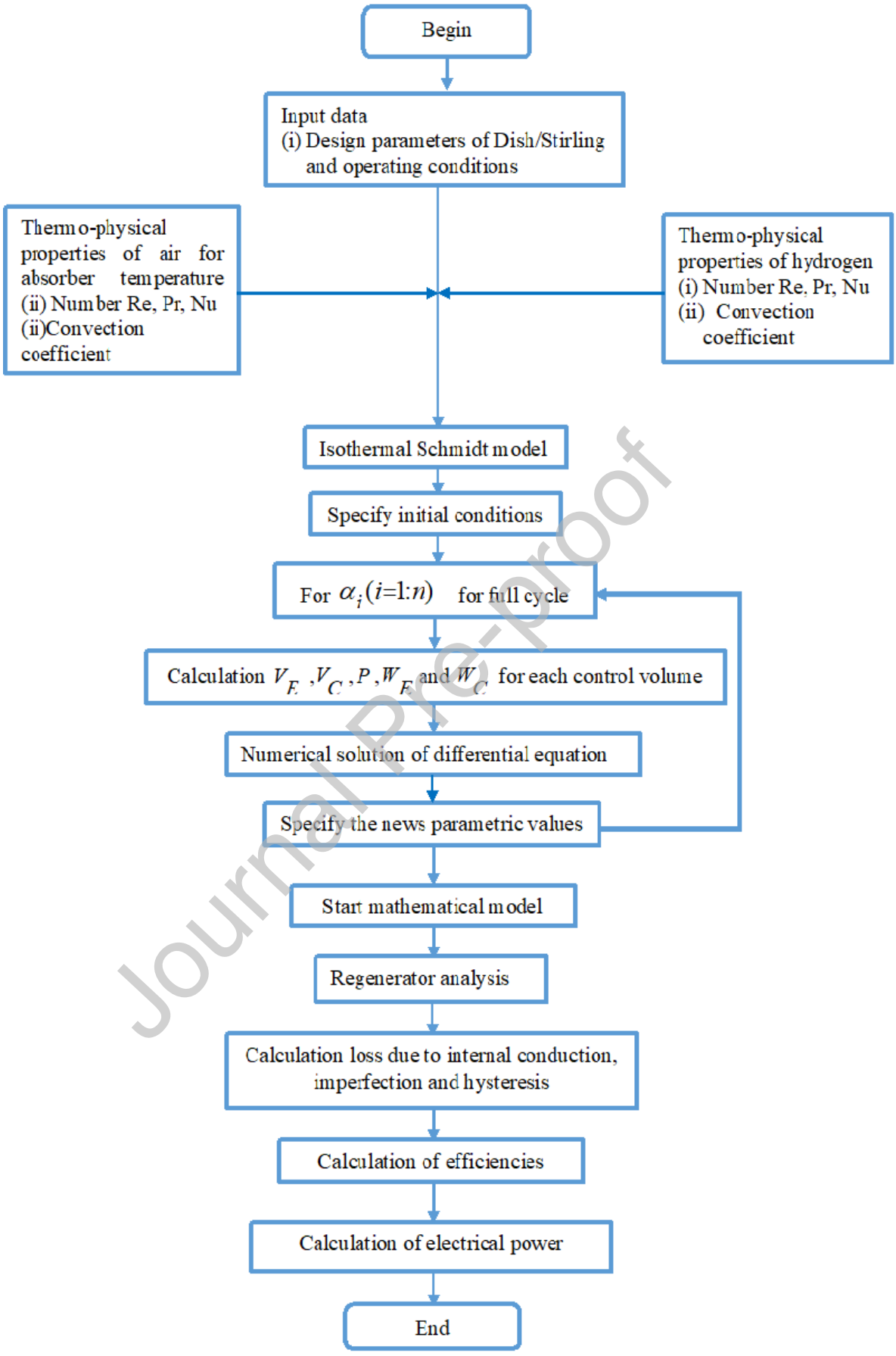

Fig 4: Resolution algorithm.

3. Validation

This section compares the results obtained with previous research data to assess their consistency.

First case

The first comparison figure shows the validation of the model with the real values of the Dish/Stirling machine by Ref [36] and the theoretical Schmidt model with perfect regenerator by Babikir et al [36]. To verify the validity of the mathematical model applied in this research, we reproduced the same initial conditions as those used in the experiment conducted by Ref [36]. Table 4 highlights the discrepancies between the performance calculated by the model and that obtained from actual measurements cited in the literature. These performances are achieved with a constant solar irradiation of 906 $W.m^{-2}$, under the operating conditions specified in Table 3, but with a difference in the working fluid, as the present model requires the use of helium as a heat transfer agent rather than hydrogen. The main discrepancy between simulation and real data concerns the representation of the Stirling engine, which is to be expected given the constraints inherent in the model used. The second discrepancy concerns the receiver, where approximations have been made, particularly with regard to the distribution of the internal energy flux and optical errors, which have been estimated from the interception factor. The difference with the work of Babikir et al [36] lies in the consideration of heat losses in the regenerator and the hysteresis power loss of the gas springs considered for modeling the Stirling engine. Since Babikir et al [36] use Schmidt's ideal model. Nevertheless, the deviations remain within reasonable limits.

Comparing the results of rudimentary Stirling engine models with experimental tests is often considered pointless due to the oversimplification of the models. These simplified models, often based on the ideal Stirling cycle, fail to take into account many of the real losses in a physical Stirling engine, such as frictional losses, conductive and radiative heat losses, and losses due to regenerator incompetence.

The 12.44% error between test data and Dish/Stirling machine models is due to the complexity of the Stirling engine and the approximations inherent in the simulation models. Stirling engines feature complex thermal and mechanical phenomena, and even the most advanced models have difficulty in accurately capturing all these details, leading to discrepancies in predictions.

Table 4: Comparative evaluation between simulation, experimental data and previous studies of Dish/Stirling subsystem performance.

Data	Theoretical modeling applied in this study.	Babikir et al [36]	Errors between model and Ref [36] (%)	Experimental measures [36]	Errors between model and experimental measures (%)
η_0	90	75	4.6	78.6	14.5

η_{elec}	25.3	21	6.7	22.5	12.44

Second case:

Table 5 compares the simulated results of the model with the numerical studies of Ref. [62]. The model is a physical realization of the parabolic concentrator model. It is found that the mathematical model of the Dish/Stirling device studied under the specified conditions is 4.38% more energy efficient than that of Ref [62]. This reveals that the proposed method outperforms that of Ref. [62] in terms of optimizing the energy efficiency of a Dish/Stirling device. Thus, the considerations of certain recurring physical phenomena, notably the losses by conduction, radiation and convection of the collector and solar receiver, as well as the losses by conduction, imperfection and hysteresis of the gas elastic elements of the Stirling engine, would improve the accuracy of the results obtained and reduce energy discrepancies.

Table 5: Confrontation with other solar Stirling electric technologies.

Electric solar	Description	Collector type	η_0 (%)	η_{elec} (%)
Alhawsawi et al. [62]	Given the many advantages of the Dish/Stirling system, this research proposes in-depth theoretical modelling and performance evaluation of a hybrid system for the combined production of electricity, heat and drinking water using Dish/Stirling technology for single-effect distillation (SHPS-DS), with the aim of optimizing tri-generation.	Dish/Stirling	94	20.92
Present work	Schmidt's imperfect regenerator is used to model the Stirling engine.	Dish/Striling	90	25.3

3.1 Model validation limits

3.1.1 Lack of experimental data

The accuracy of the Dish/Stirling simulator is hampered by the lack of crucial practical information. Strict verification procedures, including targeted experimentation and methodical data compilation, will increase the accuracy and credibility of the numerical projections obtained. The following aspects are particularly relevant:

- *Thermal losses:* Radiation, conduction and convection losses may vary according to actual environmental conditions, but models may not reflect these variations without empirical data.
- *Stirling engine characteristics:* Stirling engine performance, including conversion efficiency and specific losses, can be difficult to validate without practical testing.
- *Operating conditions:* Variations in temperature, sunshine and other environmental factors are often not available in a sufficient database, making model validation difficult.

3.1.2 System complexity

The complex interdependence between the solar concentrator and the heat engine presents significant obstacles. Simulations may omit certain nuances, but without practical verification, the reliability of the results remains uncertain and open to improvement.

3.2 Suggestions for future validation

- *Experimental Testing:* Conduct tests on a prototype Dish/Stirling system to gather data on actual performance, including heat loss and Stirling engine efficiency.
- *Longitudinal Data Collection:* Install sensors to continuously monitor system performance under various environmental conditions, in order to accumulate long-term data.
- *Comparison with Analytical Models:* Use proven analytical models to compare existing model results, identifying discrepancies and adjusting the model accordingly.
- *Collaboration with Research Institutes:* Working with specialized laboratories to validate models using sophisticated measurement equipment and technical expertise.

3.3 Uncertainty analysis and sensitivity of results

3.3.1 Uncertainty analysis

Uncertainties come from a variety of sources, including experimental measurements, approximations in models and material properties. Statistical methods, such as Monte Carlo analysis, are used to simulate the impact of uncertainties on results, by randomly drawing input parameters within their uncertainty ranges.

3.3.2 Sensitivity of results

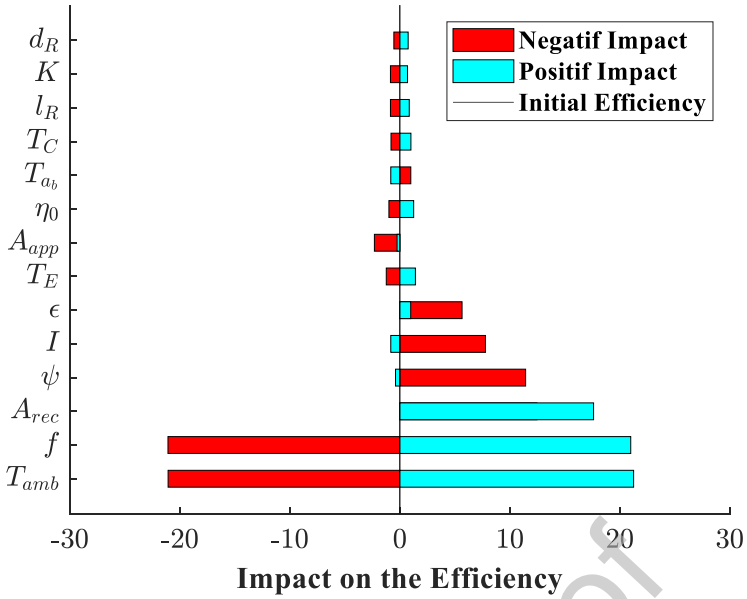

Fig 5. Impact of variations in decision variables on Dish/Stirling efficiency.

The sensitivity analysis shown in Fig. 5 reveals that parameters associated with red bars have a negative impact on efficiency, while those represented by cyan bars contribute positively. Parameters with larger amplitude bars, such as ambient temperature, Stirling engine frequency, solar receiver surface area, regenerator porosity and solar irradiation, exert a significant influence, suggesting potentially critical variations in system efficiency. Some negative impact coefficients reach -21.07%, highlighting crucial control points. By integrating these results in the context of initial efficiency, the analysis identifies risks and opportunities for improvement, informing optimization and system design strategies.

4. Results and discussion

Performance indicators are used to assess the results of the Dish/Stirling system, including solar electric energy production and overall energy efficiency. To analyze the influence of operational and design factors on the Dish/Stirling system, key parameters have been identified and summarized in Table 3. Global and optimization analyses were carried out using helium as the thermal agent. This in-depth analysis examines the simulation results, focusing on the influence of the geometric characteristics of the solar collector and receiver, as well as factors such as emissivity, optical efficiency, operating temperatures and regenerator parameters on the overall performance of the Dish/Stirling system, and presents the optimum values for maximum energy efficiency and electrical output. Computer modeling was carried out using MATLAB software, facilitating detailed numerical simulations and analysis.

4.1 Effect of absorber temperature and irradiation

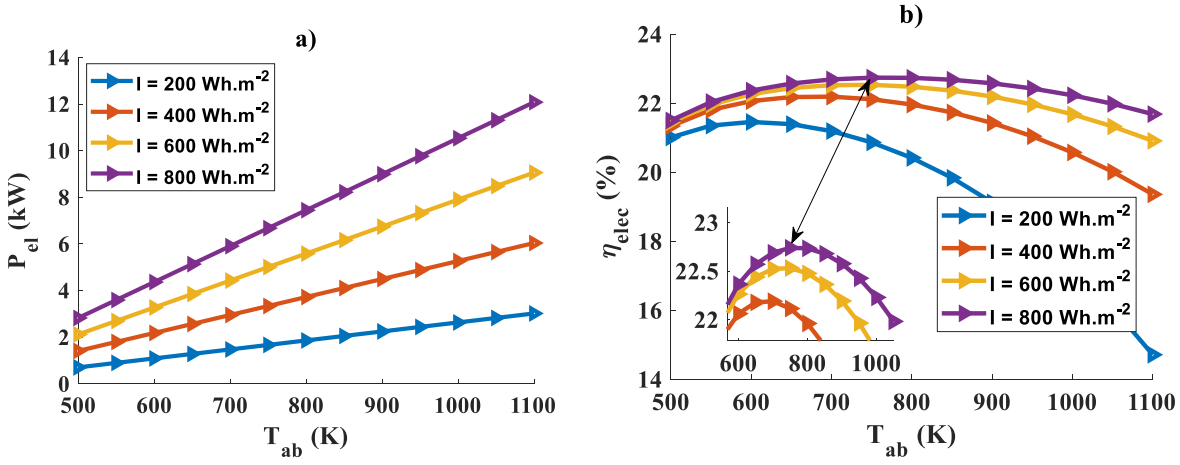

Fig 6 : Effect of absorber temperature and irradiation on a) electrical power and b) Dish/Stirling efficiency.

In **fig 6.a**, raising the absorber temperature from 500K to 1100K implies an increase in the electrical power of the parabolic concentrator of around 76% when solar irradiation is set at 800 Wh.m^{-2}. This trend can be interpreted as an optimization of the energy performance of the mechanical process, especially in plants with parabolic concentrators and Stirling engines, where productivity is closely linked to the temperature difference between the hot focus and the cold reservoir. Similarly, fluctuating solar irradiance leads to an increase in the electrical power of the parabolic concentrator from 1.29 kW to 5.14 kW at an absorber temperature of 650 K. Therefore, to improve the electrical output of the parabolic concentrator, a higher value of solar irradiation and absorber temperature would be required.

In **fig 6.b**, the increase in absorber temperature from 500 to 1100 K implies a low-speed growth of the parabolic concentrator efficiency from 21.56% to its maximum value at 22.74% for an optimum absorber temperature of 750 K, then drops at high speed to around 21.68%, when solar irradiation is stable at 800 Wh.m^{-2}. The drop in productivity at higher temperatures is mainly due to the dramatic increase in heat loss through radiative emission, in accordance with the principle of physics describing heat exchange between bodies. These heat losses take over at high temperatures and cancel out the performance advantages of the device, causing a marked reduction in overall efficiency. Whereas increasing solar irradiation from 200 Wh.m^{-2} to 800 Wh.m^{-2} leads to an optimization of the parabolic concentrator's efficiency at high speed from 20.86% to 22.11%, then increases at low speed to 22.74%. To increase the energy efficiency of the parabolic concentrator, high solar irradiation and absorber temperature would be required.

4.2 Effect of the temperature of the working fluid in the cold space or compression chamber and the emissivity factor of the solar collector

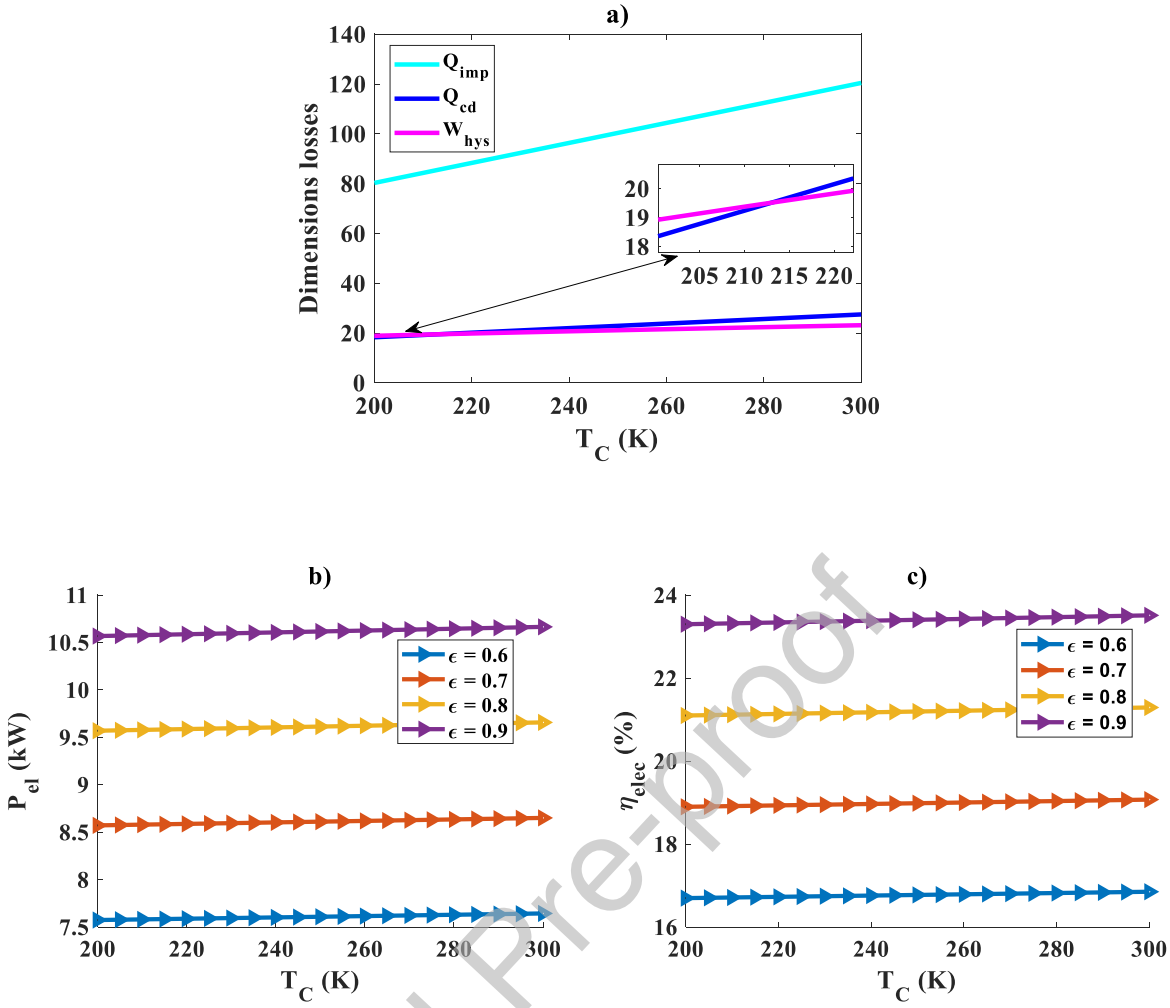

Fig 7: Effect of the temperature of the compression chamber of the Stirling engine and the emissivity factor of the solar collector b) electric solar power and c) efficiency of the system studied.

In **fig 7.b**, it can be seen that the fluctuation in helium temperature in the Stirling engine's compression zone enclosure from 200 K to 300 K involves an insignificant increase in the electrical power of the solar parabolic concentrator from 9.57 kW to 9.7 kW when the solar collector's emissivity factor is set at 0.8. This observed effect can be attributed to increases in regenerator heat loss and gas spring hysteresis power loss, as described in **fig 7.a**. Similarly, raising the emissivity factor of the solar collector from 0.6 to 0.9 leads to an optimization of the solar concentrator's electrical power from 07.64 kW to 10.67 kW when the helium temperature in the cold space is set at 300 K. To improve the electrical output of the solar parabolic concentrator, a high working gas temperature in the compression chamber of the Stirling engine and a high emissivity of the solar collector would be required.

In **fig 7.c**, the same effects observed previously on the variation of the working gas temperature and the variation of the solar collector emissivity are also observed on the energy efficiency of the solar parabolic concentrator. To improve the energy efficiency of the Dish/Stirling system, a high working fluid temperature and high solar collector emissivity would be required.

4.3 Effect of Stirling engine regenerator diameter and concentrator surface area

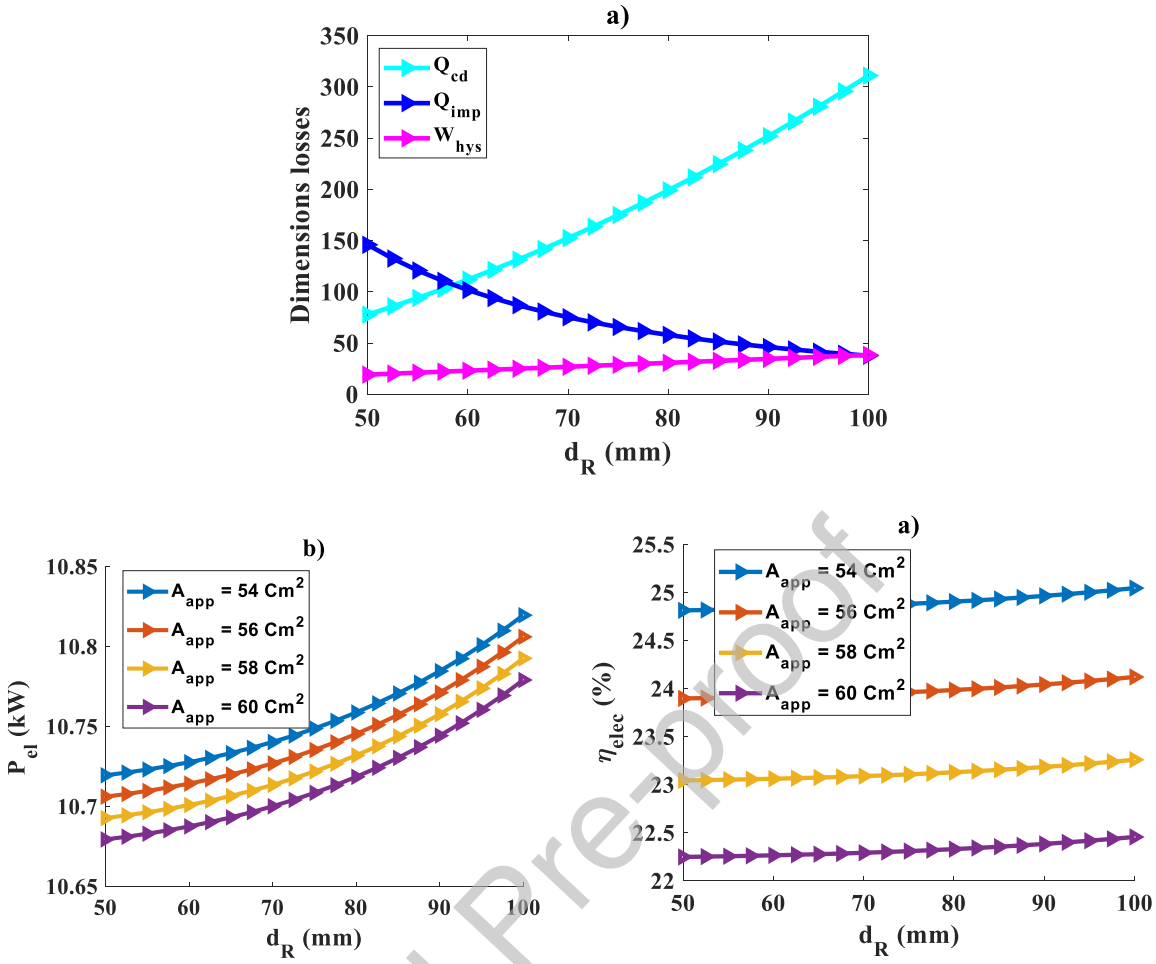

Fig 8: Effect of Stirling engine regenerator diameter and collector surface area on b) solar electric power and c) efficiency of the system studied.

In **fig 8.b**, increasing the internal diameter of the regenerator from 50 mm to 100 mm results in an insignificant increase in the electrical power of the parabolic concentrator from 10.71 kW to 10.81 kW, when the solar collector surface is 56 cm^2. This visualized effect may be due to the imperfection of the regenerator linked to the physical phenomena causing losses in its enclosure, such as the high growth of losses by thermal conduction and the low growth of power losses by hysteresis, as shown in **fig 8.a**. But increasing the area of the solar collector from 54 cm^2 to 60 cm^2, implies an insignificant decrease in the electrical power of the parabolic concentrator of 0.4%, when the internal diameter of the regenerator is fixed at 7 cm^2. This trend is probably due to the simultaneous increase in radiative losses (dispersion, misalignments, geometric distortions) that compensate for the surplus energy collected, resulting in a relatively constant efficiency. In fact, to optimize the concentrator's electrical power, a small solar collector surface area and a large internal diameter of the regenerator would be required.

Fig 8.c shows a slight increase in the energy efficiency of the parabolic concentrator from 22.25% to 22.46%, i.e. a slight increase of 0.21% for a solar collector area of 60 cm^2. This could be due to the increase in gas spring hysteresis power losses and regenerator internal

conduction heat losses, and the decrease in heat losses due to the imperfect nature of the regenerator, as shown in **fig 8.a**. The similar effects observed in **fig 8.b** on the variation of solar collector area with electrical power are also observed on energy efficiency in **fig 8.c**. Thus, to improve the energy efficiency of the Dish/Stirling system, a large internal diameter of the regenerator and a small surface area of the solar collector would be required.

4.4 Effect of Stirling engine frequency and ambient temperature

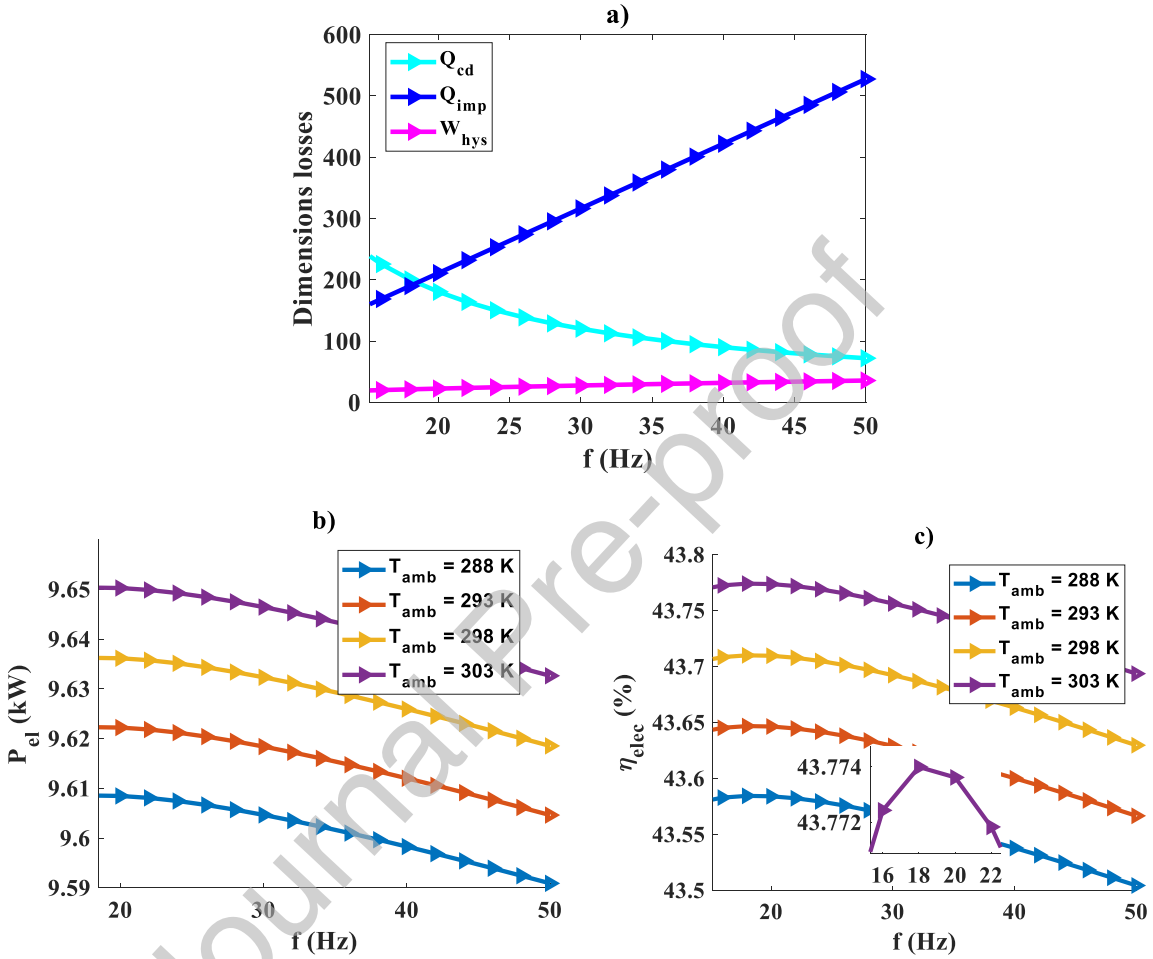

Fig 9: Effect of Stirling engine speed and ambient temperature on b) solar electric power and c) overall efficiency of the system studied.

In **fig 9.b**, the increase in Stirling engine speed from 18 Hz to 50 Hz implies an insignificant reduction in the electrical power of the parabolic solar concentrator from 9.64 kW to 9.62 kW, i.e. 0.2% at an ambient temperature of 298 K in BAZOU. This could be due to the rapid increase in heat loss through regenerator imperfections with Stirling engine speed observed in **fig 9.a**. The increase in ambient temperature from 288 K to 303 K results in an insignificant rise in electrical power from 9.6 kW to 9.64 kW when the frequency is 26 Hz. Thus, to optimize the electrical power of the parabolic concentrator, a low Stirling engine frequency and a high ambient temperature would be required.

Whereas in **fig 9.c**, increasing the Stirling engine speed from 15.5 Hz to 50 Hz implies an increase in the parabolic concentrator's energy efficiency from 43.76% to reach its peak at

43.78% when the optimal engine speed is 18 Hz, before decreasing to reach its minimum value at 43.71%, for a medium temperature of 303 K. As a result, this optimum value for Stirling engine speed coincides with the intersection of the regenerator's internal heat conduction loss and the energy loss due to the imperfect nature of the regenerator, which respectively decreases and increases with Stirling engine speed, as shown in **fig 9.a**.

4.5 Effect of Stirling engine regenerator internal length and swept volume ratio on system performance

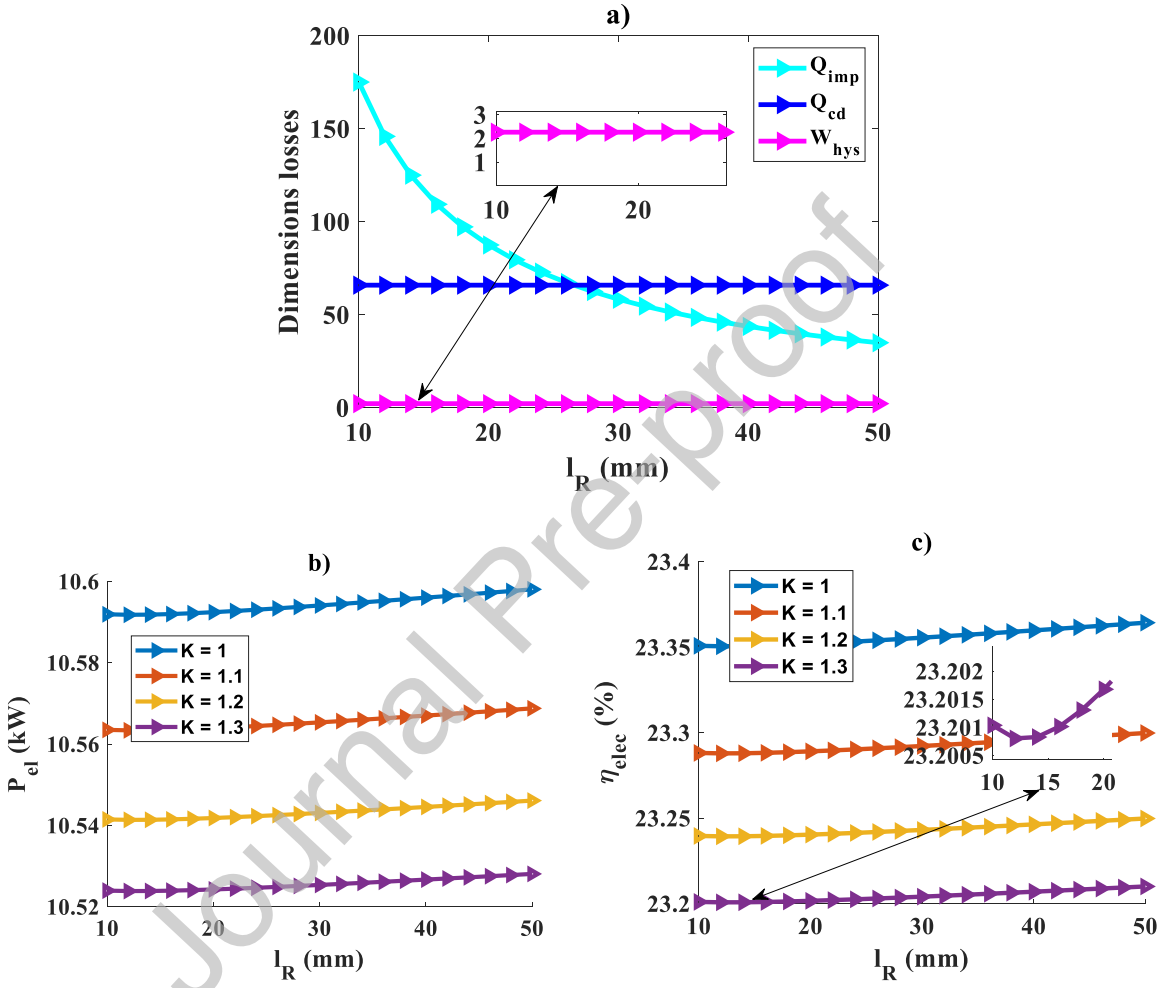

Fig 10: Effect of the internal length of the Stirling engine regenerator and the swept volume ratio on b) the solar electric power and c) the efficiency of the system studied.

As a result of the lower heat loss due to the imperfect nature of the regenerator within the Stirling engine, the temperature of the working fluid in the compression chamber increases. And the increase in heat loss through internal conduction in the regenerator and power loss through gas spring hysteresis due to the behavior of the working fluid in the expansion and compression chambers of the Stirling engine as the internal length of the regenerator increases, as shown in **fig 10.a**. The variation in electrical power observed in **fig 10.b** increases with the internal length of the regenerator. This can be explained by the fact that an increased regenerator length promotes optimum thermal restitution, which intensifies heat exchange between the helium and the thermal regenerator. And the energy efficiency

visualized in **fig 10.c** of the parabolic solar concentrator decreases until it reaches its minimum extremum at 23.2% before increasing at low speed to reach its maximum value at 23.21% when the swept volume ratio is fixed at 1.3. To optimize the parabolic solar concentrator's energy performance, we recommend a long internal regenerator length and a high swept volume ratio.

It's true that, in general, increasing the internal length of a regenerator can, under certain conditions, improve a system's electrical output and energy efficiency. However, this improvement is not always significant and depends on many factors, such as the type of system, the operating range and the specific characteristics of the regenerator. It should also be noted that increasing regenerator length is not always beneficial. Excessive lengths can lead to excessive pressure drops, manufacturing problems and higher costs. What's more, improved efficiency is often subject to a saturation point.

4.6 Effect of regenerator porosity and swept volume of the Stirling engine

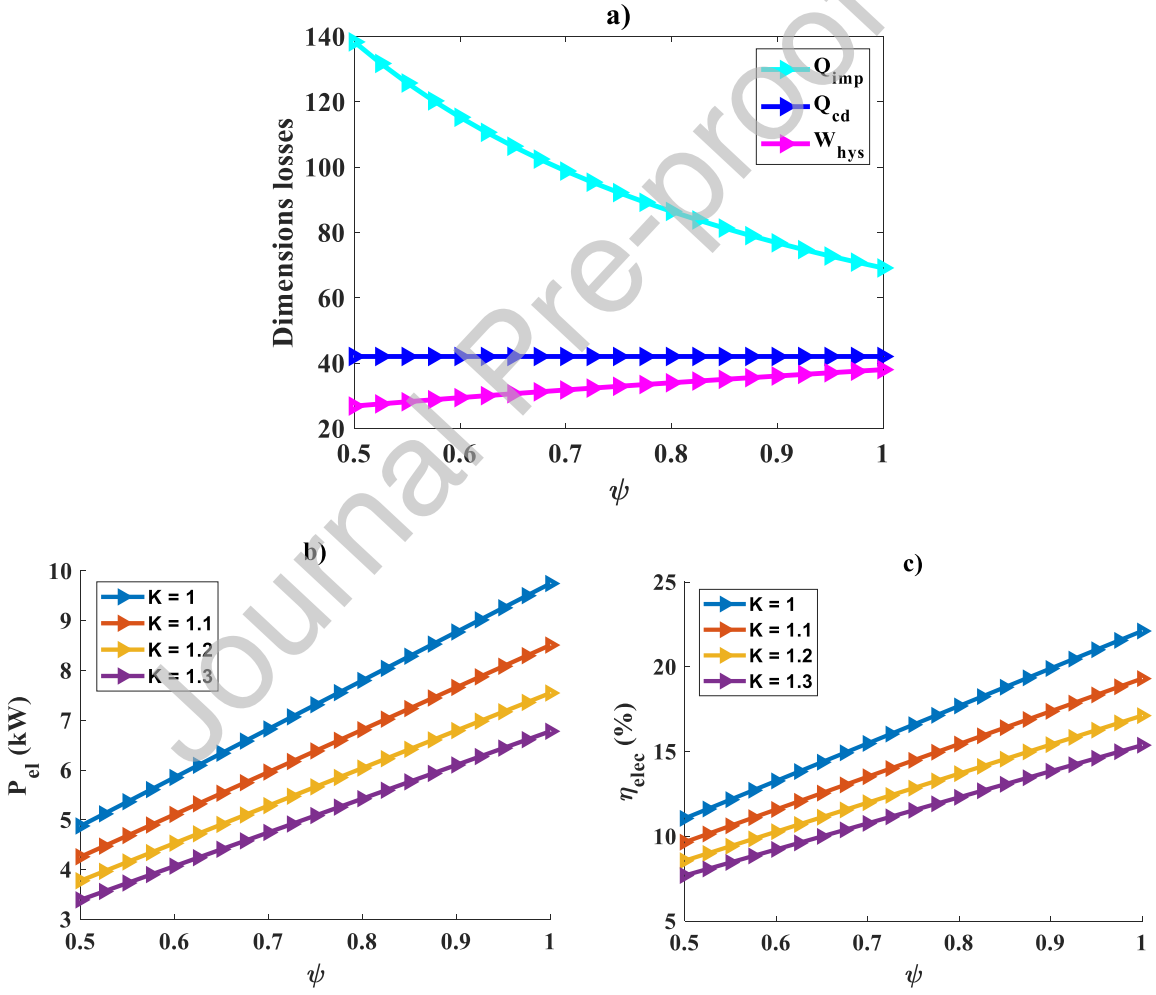

Fig 11: Effect of Stirling engine regenerator porosity and cooler swept volume ratio on b) solar electric power and c) efficiency of the system studied.

In **fig 11.b**, the increase in the porosity of the regenerator material from 0.5 to 1, results in a significant increase in the electrical power of the parabolic solar concentrator from 3.78 kW to 7.55 kW, i.e. an increase of 49.93% when the swept volume ratio is 1.2. This observed effect

may be due to the decrease in imperfection losses in the regenerator as shown in **fig 11.a**, since according to the work of Ref [33], this is the largest loss in the regenerator. Also to the reduction of pressure losses in the regenerator which improves the efficiency of thermal recovery, thus allowing a more optimal heat return to helium, which has the effect of increasing the overall efficiency of the Stirling cycle.

And increasing the swept volume ratio from 1 to 1.3, results in a reduction in electrical power at high speed from 9.261 kW to 8.086 kW, then at low speed down to 6.44 kW, when the regenerator porosity is set to 0.95. Thus, for an improvement in electrical power, a low swept volume ratio and high regenerator porosity would be required.

In **fig 11.c**, the increase in regenerator porosity from 0.5 to 1 results in a rise in energy efficiency from 7.691% to 15.38% when the swept volume ratio is 1.3. This could be due to the drop in heat loss due to regenerator imperfection towards the increase in regenerator porosity as described in **fig 11.a**. While increasing the swept volume ratio from 1 to 1.3 results in a decrease in energy efficiency at high speed from 19.9% to 17.37%, then at low speed down to 13.84%, when porosity is fixed at 0.9. Thus, to optimize energy efficiency, a high regenerator porosity and a low swept volume ratio would be required.

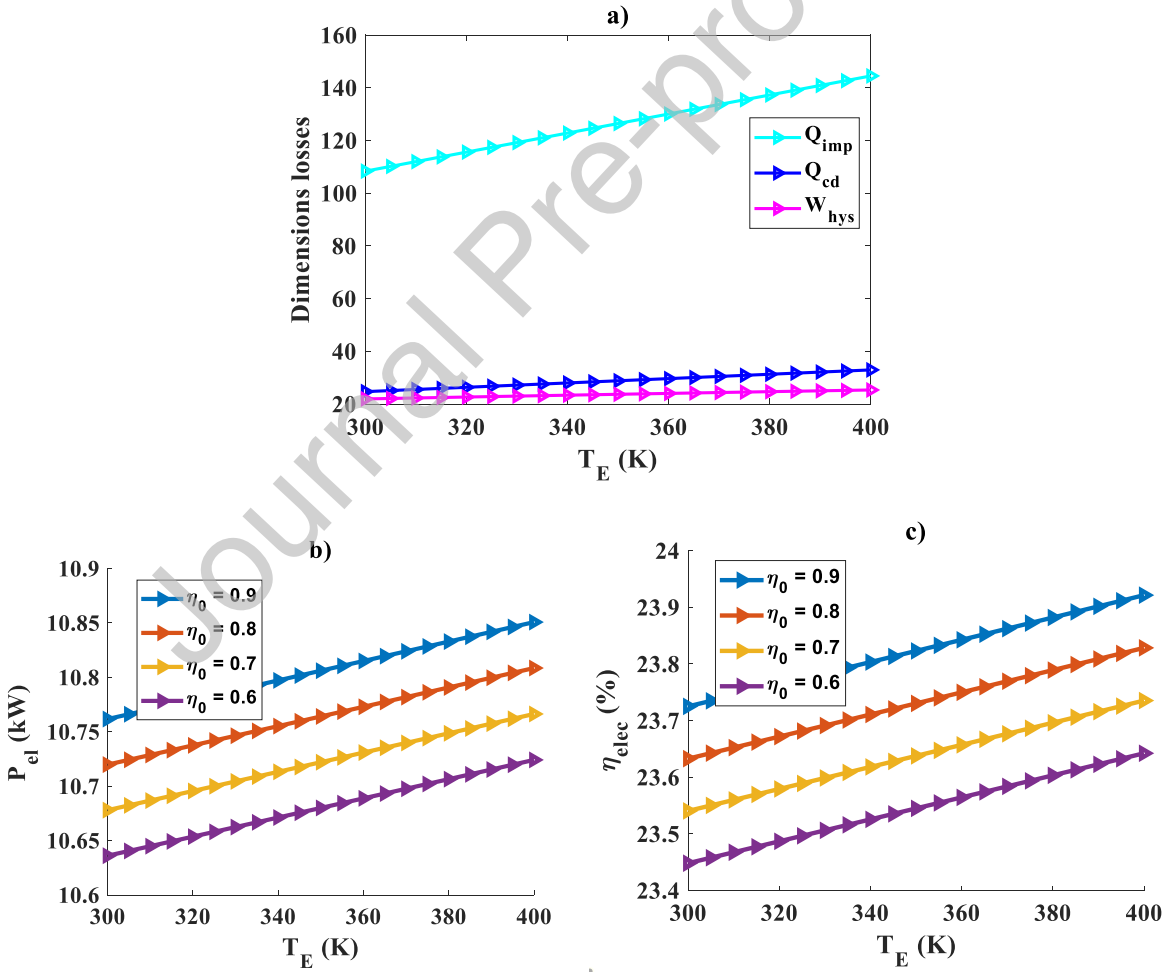

Fig 12: Effect of hot Stirling engine temperature and collector optical efficiency b) solar electric power and c) efficiency of the system studied.

In **fig 12.b**, when the hot temperature rises from 300 K to 400 K, this results in an insignificant increase in electrical power from 10.72 kW to 10.81 kW for a solar collector optical efficiency of 0.8. This could be due to the insignificant increase in regenerator heat loss and hysteresis loss, as shown in **fig 12.a**. Similarly, increasing the optical efficiency of the solar collector from 0.6 to 0.8 implies an increase in electrical output from 10.69 kW to 10.82 kW, when the hot temperature is 365 K. Thus, to optimize solar power output, a high solar collector optical efficiency and hot temperature would be required.

In **fig 12.c**, increasing the hot temperature of the Stirling engine from 300 K to 400 K improves the energy efficiency of the Dish/Stirling system from 23.63% to 23.83%, when the optical efficiency is 0.8. These observed effects could be due to the insignificant increases in conduction heat loss in the regenerator and power loss due to gas spring hysteresis visualized in **fig 12.a**. The same applies to the increase in optical efficiency from 0.6 to 0.8, which implies an increase in solar energy efficiency from 23.61% to 23.89%, when the Stirling engine expansion chamber temperature is 385 K.

4.7 Effect of absorber surface and irradiance on electrical power and system efficiency

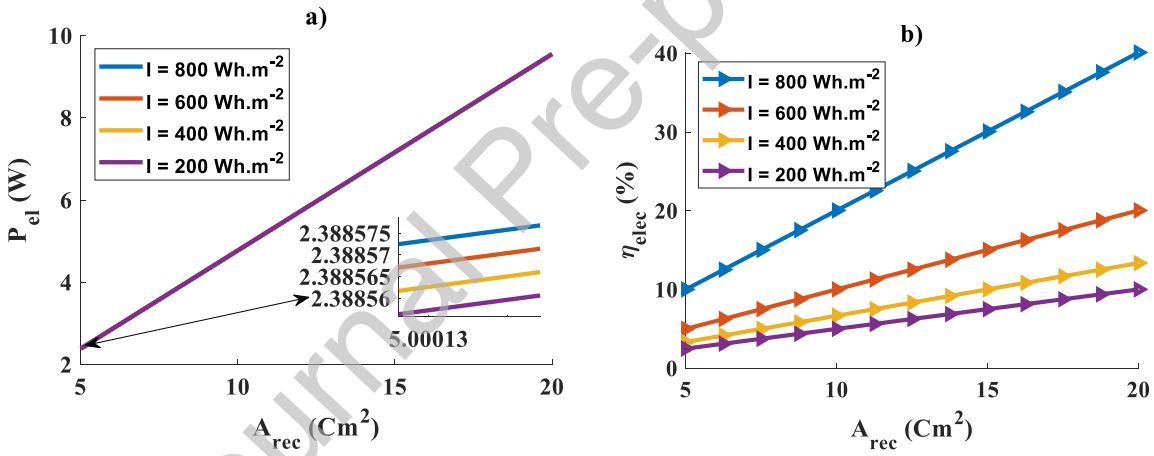

Fig 13: Effect of solar receiver surface and irradiance on a) electrical power and b) Dish/Stirling efficiency.

In **fig 13.a**, rising the solar receiver space the from 5 cm^2 to 20 cm^2 significantly increases the electrical power generated by the parabolic concentrator from 2.5 kW to 9.58 kW. This is because the larger the surface area of the solar receiver, the more solar energy it can capture. However, the increase in solar irradiation from 200 $wh.m^{-2}$ to 800 $Wh.m^{-2}$ contributes to an insignificant rise in electrical power. Thus, to optimize the electrical power of the parabolic concentrator, a large receiver surface area may be required.

Fig 13.b shows an increase in overall efficiency from 8% to 19% with rising solar receiver surface area when solar irradiation is 600 $Wh.m^{-2}$. When the surface area of the solar receiver is 20 cm^2, rising solar irradiation from 200 $Wh.m^{-2}$ to 800 $Wh.m^{-2}$ results in a significant increase in energy yield from 8% to 18% at low speed, then up to 39% at high speed.

Therefore, to improve the efficiency of the parabolic concentrator, a high solar receiver surface area and low solar irradiation would be required.

The quantitative data from the numerical simulation are compiled in Table 6, showing the key parameters analyzed and the losses recorded. With a heat loss of 820 W, the solar power generation capacity is 10.82 kW, giving an energy efficiency of 43.7%.

Table 6: Summary of simulation results

Operational parameters	**Value**
Key output parameters	
P_{elec} **(kW)**	10.85
η_{elec} (%)	43.78
Losses	
Q_{cd} **(kW)**	0.225
Q_{imp} **(kW)**	0.520
W_{hys} **(kW)**	0.075

Table 7 shows the quantitative data derived from the numerical modeling of the key performance variables evaluated, as well as the various design and operating attributes observed for the device.

Table 7: Optimal configurations.

Variables			**Objective functions**	
Parameter	**[17, 38, 41]**	**This work**	η_{elec} **(%)**	$\mathbf{P_{elec}}$ **(kW)**
T_{amb} (K)	288	303	43.78	9.650
I $(Wh.m^{-2})$	1000	800	22.74	6.676
T_{ab} (K)	1100	750	22.74	6.676
T_E (K)	320	400	23.92	10.850
T_C (K)	288	300	23.51	10.670
A_{app} (Cm^2)	56.7	54	25.05	10.820
dr (mm)	3	100	25.05	10.820
f (Hz)	25	18	43.78	9.650
l_r (mm)	6	50	23.36	10.600
η_0	0.9	0.9	23.92	10.850
A_{rec} (cm^2)	13.17	20	40.12	9.554
K	1	1	22.11	9.748

ψ	0.7	1	22.11	9.748
ε	0.9	0.9	23.51	10.670

5. Conclusion

This study presents a computer model to evaluate the energy yields of a large-scale Dish/Stirling system. This model incorporates heat loss and heat transfer mechanisms linked to imperfections and internal conduction. In addition, energy losses due to the hysteretic dependence of the gas springs of the Alpha Stirling engine and heat losses through convection, radiation and conduction from the solar concentrator are integrated to optimize the system's energy capacities, particularly for power generation at BAZOU. The key features of the parabolic concentrator for maximizing energy yield and solar electric power have been identified. The key solutions are outlined as follows:

1. For a variation in solar energy efficiency and electrical power with Stirling engine speed, the optimum frequency is 18 Hz, varying from 10 to 50 Hz, as opposed to the manufacturer's 25 Hz.
2. Rising absorber temperature significantly increases the electrical production and solar efficiency of the machine, until reaching its optimal value at 750 K.
3. Increasing the internal length of the regenerator significantly optimizes the system's electrical output and energy efficiency. In addition, a regenerator internal length of 15 mm implies poor overall efficiency performance.
4. Increasing the emissivity factor improves overall energy efficiency and solar power output.
5. Increasing the swept volume ratio reduces the electrical power and energy efficiency of the Dish/Stirling system.
6. The results provide predictive models that can be used to guide engineers in designing more efficient systems.
7. By optimizing key parameters, production and operating costs can be reduced, making the system more competitive on the energy market.

In addition, the parabolic concentrators of the Schmidt model with real regenerator achieve a high solar energy efficiency of 25.3%, surpassing the ideal model of Ref [36]. The results obtained can be used to design future concentrators with higher-performance solar dishes.
However, further research is needed to analyze the economic and technical viability of this system.
Future research directions include:
- Environmental Fluctuation Analysis: Study the impact of climatic variations on system performance to develop more robust solutions.
- Systems integration: seeking synergies between the Dish/Stirling system and other renewable energy technologies to create hybrid energy solutions.
- Advanced Optimization: Explore more sophisticated optimization algorithms, such as machine learning and the NSGA II algorithm, to further refine system configurations.

Conflict of Interest Statement

The authors declare that there are no conflicts of interest with each other or with any person or institution.

Funding Statement

This study did not receive funding from any person or institution.

CRediT authorship contribution statement

Ghislain Junior Bangoup Ntegmi: Conceptualization, Data curation, Formal analysis, Funding acquisition, Investigation, Methodology, Project administration, Resources, Software, Supervision, Validation, Visualization, Writing – original draft, Writing – review & editing. **Germaine Mabou Ninkam:** Conceptualization, Formal analysis, Funding acquisition Investigation, Visualization, Writing – original draft. **Francois Lanzetta:** Conceptualization, Data curation, Funding acquisition, Investigation, Methodology, Project administration, Software, Supervision, Validation, Visualization. **Flavian Emmanuel Sapnken:** Conceptualization, Formal analysis, Funding acquisition, Investigation, Methodology. **Mebarek-Oudina Fateh:** Conceptualization, Data curation, Formal analysis, Funding acquisition, Methodology. **Bleck Fredi Kamto Pomou:** Data curation, Funding acquisition, Investigation, Methodology, Project administration. **René Tchinda:** Investigation, Methodology, Resources, Software, Supervision, Validation.

Data availability statement

Data available on request from the authors.

Declaration of generative AI statement

When revising this manuscript, the authors used CROK AI to correct and improve the grammar.

Reference

[1] Y.F. Nassar, H.J. El-khozondar, A.A. Ahmed, A. Alsharif, M.M. Khaleel, R.J. El-Khozondar, A new design for a built-in hybrid energy system, parabolic dish solar concentrator and bioenergy (PDSC/BG): A case study–Libya, Journal of Cleaner Production 441 (2024) 140944, https://doi.org/10.1016/j.jclepro.2024.140944

[2] H.A. Khawaldeh, B. Shboul, M. Al-Smairan, M. Al-Soeidat, D. Lu, F. Almomani, Comparative Energy and Economic Analysis of Dish Stirling Engine and National Grid Electricity for Residential Building in Mafraq, Jordan, Sustainability 16 (14) (2024) 5945, https://doi.org/10.3390/su16145945

[3] S. Zare, A. Tavakolpour-Saleh, Free piston Stirling engines: A review, Int. J. Energy Res. 44 (7) (2020) 5039-5070, https://doi.org/10.1002/er.4533.

[4] J. Park, J. Ko, H. Kim, Y. Hong, H. Yeom, S. Park, S. In, The design and testing of a kW-class free-piston Stirling engine for micro-combined heat and power applications, Appl. Therm. Eng. 164 (2020) 114504, https://doi.org/10.1016/j.applthermaleng.2019.114504.

[5] S. Zhu, G. Yu, Y. Ma, Y. Cheng, Y. Wang, S. Yu, E. Luo, A free-piston Stirling generator integrated with a parabolic trough collector for thermal-to-electric conversion of solar

energy, Appl. Energy 242 (2019) 1248-1258, https://doi.org/10.1016/j.apenergy.2019.03.169.

[6] S. Zhu, G. Yu, X. Li, M. Ying, C. Yan, W. Dai, E. Luo, Acoustic field characteristics of a free-piston Stirling cryocooler with large cooling capacity at liquid nitrogen temperature, Appl. Therm. Eng. 147 (2019) 324-335, https://doi.org/10.1016/j.applthermaleng.2018.10.096.

[7] S. Qiu, Y. Gao, G. Rinker, K. Yanaga, Development of an advanced free-piston Stirling engine for micro combined heating and power application, Appl. Energy 235 (2019) 987-1000, https://doi.org/10.1016/j.apenergy.2018.11.036.

[8] Y. Qi, D. Sun, J. Zhang, Study on the thermoacoustic characteristics and acoustic matching of a 15 We free-piston Stirling generator, Appl. Therm. Eng. 235 (2023) 121357, https://doi.org/10.1016/j.applthermaleng.2023.121357.

[9] L. Kong, J. Jiang, S. Sun, H. Li, L. Shui, W. Ye, Z. Wu, Effects of internally charged hydrostatic gas bearing on performance of gas springs in free piston stirling engine, Case Stud. Therm. Eng. 61 (2024) 104925, https://doi.org/10.1016/j.csite.2024.104925.

[10] C. Perozziello, L. Grosu, B.M. Vaglieco, Free-piston stirling engine technologies and models: A review, Energies 14 (21) (2021) 7009, https://doi.org/10.3390/en14217009.

[11] X. Gao, X. Yang, D. Sun, J. Chai, Y. Quan, Performance study of 1.5 kWe free piston Stirling generator emulating solar power working conditions, Case Studies in Thermal Engineering 51 (2023) 103542, https://doi.org/10.1016/j.csite.2023.103542

[12] I. Tursunović, D. Papurello, Design of a Solar Dish Receiver and Life Cycle Assessment of a Hot Water System, Clean Technologies 6 (1) (2024) 379-396, https://doi.org/10.3390/cleantechnol6010019

[13] M.H. Ahmadi, S. Dehghani, A.H. Mohammadi, M. Feidt, M.A. Barranco-Jimenez, Optimal design of a solar driven heat engine based on thermal and thermo-economic criteria, Energy Conversion and Management 75 (2013) 635-642, https://doi.org/10.1016/j.enconman.2013.07.078

[14] E. Bani-Hani, M.E. HajAssad, M. Tawalbeh, B. Yousef, A. Sedaghat, Enhancing cooling system of a combustion engine by integrating with a stirling cycle, Energy Engineering 116 (3) (2019) 41-53, doi: 10.1080/01998595.2019.12057061

[15] M.H. Babikir, D. Njomo, M.Y. Khayal, H.D. Temene, D.T. Joel, Estimation of direct solar radiation of Chad, Energy and Power Engineering 10 (5) (2018) 212-225, https://doi.org/10.4236/epe.2018.105015

[16] M.H. Babikir, D. Njomo, M. Barka, M.Y. Khayal, D. Goron, V.S. Chara-Dackou, N.S. Elie, Modeling the incident solar radiation of the city of N'Djamena (Chad) by the Capderou method, International Journal of Photoenergy 2020 (1) (2020) 6292147, https://doi.org/10.1016/j.rineng.2024.102443

[17] A. Khosravi, R.O. Nunes, M.E.H. Assad, L. Machado, Comparison of artificial intelligence methods in estimation of daily global solar radiation, Journal of Cleaner Production 194 (2018) 342-358, https://doi.org/10.1016/j.jclepro.2018.05.147

[18] J. Kitmo, G.B. Tchaya, N. Djongyang, Optimization of hybrid grid-tie wind solar power system for large-scale energy supply in Cameroon, International Journal of Energy and Environmental Engineering 14 (4) (2023) 777-789, https://doi.org/10.1080/01430750.2024.2351089

[19] A. Khosravi, S. Syri, J.J. Pabon, O.R. Sandoval, B.C. Caetano, M.H. Barrientos, Energy modeling of a solar dish/Stirling by artificial intelligence approach, Energy Conversion and Management 199 (2019) 112021, https://doi.org/10.1016/j.enconman.2019.112021

[20] M.E. Zayed, J. Zhao, W. Li, A.H. Elsheikh, Z. Zhao, A. Khalil, H. Li, Performance prediction and techno-economic analysis of solar dish/stirling system for electricity generation, Applied Thermal Engineering 164 (2020) 114427, https://doi.org/10.1016/j.applthermaleng.2019.114427

[21] B.E.K. Nsafon, A.B. Owolabi, H.M. Butu, J.W. Roh, D. Suh, J.S. Huh, Optimization and sustainability analysis of PV/wind/diesel hybrid energy system for decentralized energy generation, Energy Strategy Reviews 32 (2020) 100570, https://doi.org/10.1016/j.esr.2020.100570

[22] M.E. Zayed, J. Zhao, A.H. Elsheikh, Z. Zhao, S. Zhong, A.E. Kabeel, Comprehensive parametric analysis, design and performance assessment of a solar dish/Stirling system, Process Safety and Environmental Protection 146 (2021) 276-291, https://doi.org/10.1016/j.psep.2020.09.007

[23] H. Allouhi, A. Allouhi, A. Jamil, Multi-objective optimization of a CSP-based dish Stirling field layout using Genetic Algorithm and TOPSIS method: Case studies in Ouarzazate and Madrid, Energy Conversion and Management 254 (2022) 115220, https://doi.org/10.1016/j.enconman.2022.115220

[24] Y. Tong, L. Duan, M. Yang, Y. Jiang, Performance analysis and optimization study of a new supercritical CO2 solar tower power generation system integrated with steam Rankine cycle, Applied Thermal Engineering 232 (2023) 121050, https://doi.org/10.1016/j.applthermaleng.2023.121050

[25] A. Alhawsawi, M.E. Zayed, E. Moustafa, E. Banoqitah, A.H. Elsheikh, Hybridizing solar dish Stirling power system with single-effect desalination for sustainable electricity and freshwater co-generation: Mathematical modeling and performance evaluation, Case Studies in Thermal Engineering 45 (2023) 102997, https://doi.org/10.1016/j.csite.2023.102997

[26] M. Faheem, L. Jizhan, M.W. Akram, M.U. Khan, P. Yongphet, M. Tayyab, M. Awais, Design optimization, fabrication, and performance evaluation of solar parabolic trough collector for domestic applications, Energy Sources, Part A: Recovery, Utilization, and Environmental Effects 46 (1) (2024) 13896-13915, https://doi.org/10.1080/15567036.2020.1806407

[27] N.E. Choukri, A. Azzaoui, S. Touili, A.I. Amrani, A. Alami Merrouni, Solar Dish Stirling Technology to Decrease the Grid-Electricity Dependence for Rural Communities: Case Study of Eastern Morocco, Proceedings of the 4th International Conference on Electronic Engineering and Renewable Energy Systems (2024) 389-397, https://link.springer.com/chapter/10.1007/978-981-97-9975-6_38

[28] M.E. Zayed, A.S. Menesy, A.N. Allam, S. Rehman, K. Irshad, J. Zhao, A.E. Kabeel, Design and implementation of solar dish Stirling system for smart grid power generation, Microgrid Technology and Microgrid Cluster Development (2025) 127-152, https://doi.org/10.1016/B978-0-443-13685-6.00010-0

[29] https://re.jrc.ec.europa.eu/pvg_tools/fr/

[30] A. Oudrane, B. Aour, M. Hamouda, The Implementation of Numerical Codes for the Analysis of Solar Flux Inputs and the Optimization of Thermal Comfort for a Monobloc Habitat, European Journal of Computational Mechanics 31 (02) (2022) 155-196, https://doi.org/10.13052/ejcm2642-2085.3121

[31] G.J. Bangoup Ntegmi, R. Tchinda, E. Simo, M.H. Babikir, D.R. Kamta Legue, H. Chopkap Noume, V.S. Chara-Dackou, A.Z. Kenfack, Energy and exergo-environmental performance analysis of a Stirling micro-fridge with imperfect regenerator, International Journal of Ambient Energy 45 (2024), https://doi.org/10.1080/01430750.2024.2351089

[32] Z. Zheng, Y. Chen, X. Chen, B. Shen, X. Xiao, S. Jiang, Y. Lei, Hybrid energy transmission for liquefied shale gas and electricity using cryogenic and superconducting technologies: A technical and economic study of Sichuan, China, Fuel 333 (2023) 126333, https://doi.org/10.1016/j.fuel.2022.126333.

[33] S. Bégot, M. Getie, F. Lanzetta, M. Barthès, M. de Labachelerie, A novel model and design of a MEMS Stirling cooler for local refrigeration, E3S Web of Conferences 313 (2021) 10001, https://doi.org/10.1051/e3sconf/202131310001

[34] G.J.B. Ntegmi, V.S. Chara-Dackou, M.H. Babikir, D. Awakem, H. Chopkap, E. Simo, R. Tchinda, Energy and exergo-environmental analysis of a refrigerator-Stirling/Photovoltaic system for cold production, Results in Engineering 22 (2024) 102443, https://doi.org/10.1016/j.rineng.2024.102443

[35] G.J.B. Ntegmi, M.H. Babikir, V.S. Chara-Dakou, H.N. Chopkap, O. Mounkang, A.Z. Kenfack, R. Tchinda, Thermo-economic and environmental analysis of a Dish-Stirling/Stirling thermal solar refrigerator for cold production, Renewable and Sustainable Energy Reviews 216 (2025) 115701, https://doi.org/10.1016/j.rser.2025.115701

[36] M.H. Babikir, V.S. Chara-Dackou, D. Njomo, M. Barka, M.Y. Khayal, D.R.K. Legue, J.P. Gram-Shou, Simplified modeling and simulation of electricity production from a dish/stirling system, International Journal of Photoenergy 2020 (1) (2020) 7398496, https://doi.org/10.1155/2020/7398496

[37] Berchowitz, D. M., & Urieli, I. (1984). Stirling cycle engine analysis. *Adam Hilger Ltd, Bristol*

[38] T.A. Minale, F. Lanzetta, S. Bégot, B.T. Admassu, S. Djetel-Gothe, Review on the technological advancement of Stirling cycle heat pumps, Energy Reports 12 (2024) 3504-3518, https://doi.org/10.1016/j.egyr.2024.09.028

[39] S. Koyanagi, Y. Tanimura, Classical and quantum thermodynamics in a non-equilibrium regime: Application to thermostatic Stirling engine, The Journal of Chemical Physics 161 (11) (2024), https://doi.org/10.1063/5.0220685

[40] S. Koyanagi, Y. Tanimura, Thermodynamic quantum Fokker–Planck equations and their application to thermostatic Stirling engine, The Journal of Chemical Physics 161 (11) (2024), https://doi.org/10.1063/5.0225607

[41] K. Bataineh, Hybrid fuel-assisted solar-powered Stirling engine for combined cooling, heating, and power systems: A review, Energy 297 (2024) 131506, https://doi.org/10.1016/j.energy.2024.131506

[42] S. Laín, V. Villamil, J.R. Vidal, CFD Simulation of Stirling Engines: A Review, Processes 12 (11) (2024) 2360, https://doi.org/10.3390/pr12112360

[43] W. Ye, W. Wang, H. Long, S. Sun, L. Kong, Effect of thermodynamic-dynamic parameters on the oscillation and performance of a free piston Stirling engine, Applied Thermal Engineering 253 (2024) 123845, https://doi.org/10.1016/j.applthermaleng.2024.123845

[44] D. Wang, D.J. Jasim, M. Zoghi, H. Habibi, Optimized multi-criteria performance of a poly-generation layout including a Stirling engine and a supercritical Brayton cycle using biogas and methane as two potential fuels of a topping gas turbine cycle, Energy 310 (2024) 133172, https://doi.org/10.1016/j.energy.2024.133172

[45] F. Xin, B. Xu, D. Dai, W. Liu, Z. Liu, Evaluation of heat transfer enhancement effect at the hot/cold end of a Stirling engine using performance improvement factor, Energy 311 (2024) 133351, https://doi.org/10.1016/j.energy.2024.133351

[46] F. Takemura, M. Senga, S. Hasegawa, Experimental demonstration of a liquid piston stirling engine with a wet regenerator, Applied Thermal Engineering (2024) 124660, https://doi.org/10.1016/j.applthermaleng.2024.124660

[47] J. Wang, C. Liu, H. Feng, B. Jia, Z. Zhang, Y. Wei, Transient dynamic cycle evolution and thermodynamic performance analysis of a free-piston engine generator, Energy (2024) 133669, https://doi.org/10.1016/j.energy.2024.133669

[48] M.Z. Getie, F. Lanzetta, S. Bégot, B.T. Admassu, S. Djetel-Gothe, A non-ideal second order thermal model with effects of losses for simulating Beta-type Stirling refrigerating machine, International Journal of Refrigeration 130 (2021) 413-423, https://doi.org/10.1016/j.ijrefrig.2021.05.018

[49] H. Wang, Y. Chen, J. Luo, L. Zhang, H. Kang, E. Luo, S. Zhu, A novel high-power free-piston stirling engine generator with integrated heat pipes for thermal-to-electric conversion of clean energy, Energy 314 (2025) 134218, https://doi.org/10.1016/j.energy.2024.134218

[50] J. Chai, X. Yang, X. Gao, X. Zhang, C. Li, Effects of thermodynamic parameters on thermoacoustic characteristics of free-piston Stirling engine, Applied Thermal Engineering (2025) 126181, https://doi.org/10.1016/j.applthermaleng.2025.126181

[51] S. Guo, Y. Lan, G. Li, Design and optimization of a 500 kW multi-cylinder double-acting free piston stirling engine for deep-sea nuclear power system, Progress in Nuclear Energy 180 (2025) 105588, https://doi.org/10.1016/j.pnucene.2024.105588

[52] F. Lanzetta, Regenerative stirling machines for the production of work, heating and cooling: thermo-physical phenomena and technological considerations, Proceedings of CONV-22: Int. Symp. on Convective Heat and Mass Transfer (2022), https://doi.org/10.1615/ICHMT.2022.CONV22.100.

[53] F. Lanzetta, A. Vaudrey, P. Baucour, A new method to optimise finite dimensions thermodynamic models: application to an irreversible Stirling engine, International Journal of Ambient Energy 39 (4) (2018) 392-405, https://doi.org/10.1080/01430750.2017.1310134

[54] Q. Zhou, Y. Chen, S. Sheng, Y. Wang, T. He, T. Jin, Experimental study on a wet thermoacoustic Stirling engine for water pumping, Applied Thermal Engineering (2025) 125558, https://doi.org/10.1016/j.applthermaleng.2025.125558

[55] J. Kropiwnicki, Low temperature rotary Stirling engine: Conceptual design and theoretical analysis, Applied Thermal Engineering 257 (2024) 124276, https://doi.org/10.1016/j.applthermaleng.2024.124276

[56] H. Sun, Q. Jin, G. Yu, S. Zhu, E. Luo, Experimental and numerical study on the mechanical inconsistency of a dual-opposed free-piston Stirling engine generator, Energy 315 (2025) 134432, https://doi.org/10.1016/j.energy.2025.134432

[57] G.J. Bangoup Ntegmi, F. Lanzetta, B.B. Tamegue, W.W. Nyamsi, M.H. Babikir, R. Tchinda, Impact of Enthalpy on the Exergo-environmental and Energy Performance of a Biomass Power Plant, American Journal of Physics and Applications 13 (05) (2025), https://doi.org/10.11648/j.ajpa.20251305.11

[58] D. Dai, Z. Liu, F. Yuan, R. Long, W. Liu, Finite time thermodynamic analysis of a solar duplex Stirling refrigerator, Applied Thermal Engineering 156 (2019) 597-605, https://doi.org/10.1016/j.applthermaleng.2019.04.098

[59] P.D. Li, G.Y. Ding, J.Q. Zhang, Q. Yuan, S.Q. Dai, T.H. Cui, M. Feng, Experimental demonstration of single-spin Stirling engine cycles with enhanced efficiency, Physical Review A 111 (1) (2025) L010203, https://doi.org/10.1103/PhysRevA.111.L010203

[60] A. Allouhi, T. Kousksou, A. Jamil, P. Bruel, Y. Mourad, Y. Zeraouli, Solar driven cooling systems: An updated review, Renewable and Sustainable Energy Reviews 44 (2015) 159-181, https://doi.org/10.1016/j.rser.2014.12.014

[61] L. Yaqi, H. Yaling, W. Weiwei, Optimization of solar-powered Stirling heat engine with finite-time thermodynamics, Renewable Energy 36 (1) (2011) 421-427, https://doi.org/10.1016/j.renene.2010.06.037.

[62] N. Taylor, A. Martinez, N. Alexandris, O. Gounari, S. Szabo, A. Chatzipanagi, L. Mercado, A. Falangas, European Commission. Photovoltaics Geographical Information System: Status Report 2024, (2025), https://doi:10.2760/2979595.

Nomenclature

Symboles

A	heat transfer area, m^2
A_{mat}	regenerator matrix area, m^2
C	collector concentrating ratio
d	diameter, m
f	frequency, Hz
h	conduction/convection coefficient, $W.m^{-2}.K^{-1}$
h_f	forced convection heat transfer coefficient (fluid), $W.m^{-2}.K^{-1}$
I	direct solar flux intensity, $W.m^{-2}$
kg	wall thermal conductivity, $W.K^{-1}.m^{-1}$
L	length, m
m	mass of working gas, kg

M	molecular mass, kg
Nr	engine rotation speed, $tr.mn^{-1}$
P	pressure, Pa
P_{el}	output power, kW
P_{mean}	mean pressure, Pa
Q_{cd}	power loss by conduction per cycle, kW
Q_{imp}	power loss by regenerator imperfection, kW
T	temperature, K
V	volume, m^3
V_{cm}	clearance volume of hot-source, m^3
V_{em}	clearance volume of cold-source, m^3
V_{cb}	swept volume of compression, m^3
V_{eb}	swept volume of cold-source, m^3
W	total engine work input per cycle, J
$\dot{W}_{hys}$	hysteresis, kW
Greek symbols	
α	crank angle, rad
χ	phase angle, rad
δ	stefan's constant, $W.m^{-2}.K^{-4}$
ε	emissivity factor of the collector
φ	porosity
η_0	collector optical efficiency
τ	compression ratio
ϖ	dead volume rate of compression and expansion chamber
Subscripts	
ab	absorbeur
amb	ambiant
C	compression
E	expansion
h	heater
k	cooler
R	regenerator

Conflict of Interest Statement

The authors declare that there are no conflicts of interest with each other or with any person or institution